Technical Report

TR-03-02

Gas migration in KBS-3 buffer bentonite

Sensitivity of test parameters to experimental boundary conditions

J F Harrington, S T Horseman
British Geological Survey

January 2003

Svensk Kärnbränslehantering AB
Swedish Nuclear Fuel
and Waste Management Co
Box 5864
SE-102 40 Stockholm Sweden
Tel 08-459 84 00
+46 8 459 84 00
Fax 08-661 57 19
+46 8 661 57 19

Gas migration in KBS-3 buffer bentonite

Sensitivity of test parameters to experimental boundary conditions

J F Harrington, S T Horseman
British Geological Survey

January 2003

Keywords: Gas migration, breakthrough pressure, bentonite, buffer, clay, swelling pressure, capillary pressure, permeability, preferential pathways, self-sealing, radioactive waste, repository.

Executive summary

In the current Swedish repository design concept, hydrogen gas can be generated inside a waste canister by anaerobic corrosion of the ferrous metal liner. If the gas generation rate exceeds the diffusion rate of gas molecules in the buffer porewater, gas will accumulate in the void-space of a canister until its pressure becomes large enough for it to enter the bentonite as a discrete gaseous phase. Three long term gas injection tests have been performed on cylinders of pre-compacted Mx80 bentonite. Two of these tests were undertaken using a custom-designed constant volume and radial flow (CVRF) apparatus. Gas was injected at a centrally located porous filter installed in the clay before hydration. Arrangements were made for gas to flow to three independently monitored sink-filter arrays mounted around the specimen. Axial and radial total stresses and internal porewater pressures were continuously monitored. Breakthrough and peak gas pressures were substantially larger than the sum of the swelling pressure and the external porewater. The third test was performed using an apparatus which radially constrains the specimen during gas flow. Observed sensitivity of the breakthrough and peak gas pressures to the test boundary conditions suggests that gas entry must be accompanied by dilation of the bentonite fabric. In other words, there is a tendency for the volume of the specimen to increase during this process.

The experimental evidence is consistent with the flow of gas along a relatively small number of crack-like pathways which propagate through the clay as gas pressure increases. Gas entry and breakthrough under constant volume boundary conditions causes a substantial increase in the total stress and the internal porewater pressure. It is possible to determine the point at which gas enters the clay by monitoring changes in these parameters. Localisation of gas flow within multiple pathways results in non-uniform discharge rates at the sinks. When gas injection stops, the gas pressure in the clay drops rapidly and then continues to decrease slowly with time. The transient provides clear evidence of discrete gas pathway ‘sealing’ events. Gas flow must cease when excess gas pressure (i.e. relative to porewater pressure) falls below the capillary pressure. The capillary pressure for bentonite is shown to be approximately equal to the swelling pressure. There is no evidence from these long-term tests that the development of gas pathways in any way compromises the sealing capacity of the bentonite barrier.

This report describes laboratory experimental studies performed under SKB Purchase Orders 959/1, 3140, 4565 and 5469.

Sammanfattning

I det svenska förvarskonceptet kan vätgas bildas inuti i avfallskapsel som en följd av anaerobisk korrosion av gjutjärnsinsatsen. Om gasproduktionen överstiger den diffusiva transportkapaciteten för löst gas i buffertens porvatten kommer gas att ansamlas i tomrummet i kapseln till gastrycket blir tillräckligt för att gasen ska kunna tränga in i bentoniten som en separat gasfas. Tre långtidsexperiment har genomförts med gasinjektioner i MX-80 bentonit. Två av dess har genomförts med en specialdesignad konstant volym- och radiellflödesapparat (CVRF). Gas injekterades i ett centralt poröst filter vilket var installerat i leran före bevätning. Gas kunde strömma till tre oberoende sänkor runt provet. Axiellt och radiellt totaltryck samt internt porvattentryck mättes kontinuerligt. Genombrotts- och maximalt gastryck var avsevärt högre än summan av svälltryck och externt vattentryck. Det tredje försöket gjordes med en utrustning som begränsar provet radiellt medan gasen flödar. Genbrotts- och maximalt tryck är starkt beroende på randvillkoren i försöken. Detta tolkas som att bentoniten måste utvidgas när gas tränger in. Med andra ord, provets volym måste öka under gastransport-processen.

De experimentella bevisen överensstämmer med bilden av att gas strömmar i ett begränsat antal spricklika transportvägar, vilka skapas när gastrycket ökar. Gasinträngning och genombrott vid konstant volym orsakar en påtaglig ökning av totaltrycket och det interna porvattentrycket. Det är möjligt att bestämma när gas går in i bentoniten genom att följa förändringar i dessa parametrar. Fördelningen av gas mellan olika transportvägar ger att gasflödet skiljer mellan de olika sänkorna. När gasflödet stängs av sjunker trycket i leran först snabbt och sedan fortsätter trycket att långsamt sjunka. Transienten visar klara bevis för att diskreta tranportvägar “stängs”. Gasflödet måste upphöra när gasövertrycket (relativt porvattentrycket) faller under kapillärtrycket. Kapillärtrycket för bentonit är ungefär lika med svälltrycket. Det finns inget i dessa experiment som tyder på att gastransporten skulle kunna påverka bentonitens isolerande funktion.

Contents

1 Introduction

In the Swedish KBS-3 repository concept, copper/steel canisters containing spent nuclear fuel will be placed in large diameter disposal boreholes drilled into the floor of the repository tunnels. The space around each canister will be filled with pre-compacted bentonite blocks. Over time, the bentonite blocks will draw in the surrounding groundwater and swell, closing up any construction joints. Because of the important buffering effect of the bentonite on the local water chemistry, this barrier is usually referred to as the bentonite buffer. The copper/steel waste canisters are expected to have a very substantial life in the repository environment. However, for the purposes of performance assessment, one must consider the possible impact of penetration of the canisters by water.

Assuming that available oxygen has been flushed out of the repository or consumed in chemical reactions, corrosion of the steel inner of each canister under anoxic conditions will lead to the formation of hydrogen. Radioactive decay of the waste and the radiolysis of water will produce some additional gas. Depending on the gas production rate and the rate of diffusion of gas molecules in the pores of the bentonite, it is possible that gas will accumulate in the void-space of each canister /Horseman, 1996; Horseman et al, 1997, 1999/. Gas will then enter the buffer when the gas pressure exceeds the entry pressure of the bentonite.

The currently specified bentonite for buffer construction in a Swedish repository is Mx-80 bentonite supplied by Volclay, which is a subsidiary of the American Colloid Company. Mx-80 is a naturally occurring Na-bentonite mined in Wyoming and South Dakota. It is reported to contain 65–85% of the smectite mineral montmorillonite, together with feldspars, gypsum, calcite, quartz, organics and traces of other minerals.

Key questions on gas migration arising from the Swedish KBS-3 repository concept include: (a) at what minimum gas pressure will hydrogen enter the buffer clay?; (b) how much of the buffer clay porewater will be displaced by gas?; (c) will gas flow be dispersed or focused along ‘preferential pathways’?; (d) what will control the direction of the gas flux?; (e) what will be the maximum gas pressure that developed in the buffer?; (f) will the gas have any deleterious effects on barrier performance?; and (g) what effect will the boundary condition (constant stress or constant volume) have on the gas transport behaviour?

.

2 Previous studies

The earliest papers on gas migration in clay relating to radioactive waste disposal were published by Pusch and co-workers in Sweden. Saturated Mx-80 bentonite was used in the experiments. /Pusch and Forsberg, 1983/ examined the gas permeability of this clay after gas breakthrough. The degree of saturation of specimens after the passage of the gas through the clay was found to be close to 100%, suggesting that the gas must have passed through a small number of discrete pathways. /Pusch et al, 1985/ performed eight tests on saturated Mx-80 specimens with a dry density in the range 1.1 to 1.8 $Mg.m^{-3}$. Gas pressure was increased incrementally at one to five day intervals. Gas was observed to pass into the bentonite at some critical value of pressure. These researchers noted that the critical pressure was of the same order of magnitude as the swelling pressure. /Pusch et al, 1987/ also quoted data on the gas breakthrough pressures of saturated Mx-80 from a research report published in Swedish.

/Hokari et al, 1997/ undertook gas migration experiments on compacted mixtures of sand and bentonite. The bentonite was Kunigel VI supplied by Kunimine Industries Co. Ltd. of Japan. The filler was a terrace deposits sand. The bentonite content of the specimens was typically 15%. The raw materials were mixed and then compacted at optimum water content (around 14.6%) in a mould using a rammer in a way similar to that used in Proctor compaction. A dry density of around 1.80 $Mg.m^{-3}$ was obtained using this method. The saturation procedure involved injecting water into samples at a pressure of 20 kPa. The test apparatus comprised a cylindrical cell fitted with upper and lower porous filters. The specimen was laterally constrained by the cell. Hydraulic conductivity (to water) was measured using the constant head method. Although the results show some variability, a typical value for the hydraulic conductivity of the mixture is 1×10^{-11} $m.s^{-1}$. This is equivalent to an intrinsic permeability of 1×10^{-18} m^2. Before starting a gas migration experiment, the upper porous filter was replaced by a slotted acrylic disc to allow emergent gas to be visually detected. The lower porous disc was dried. A gas pressure of 10 kPa was applied to the bottom disc causing water to be expelled from the upper face. Gas pressure was increased in increments of 10 kPa when the flow of water had ceased. After the breakthrough, gas flow rate was measured at a number of gas pressures to determine the gas permeability.

The threshold pressure in these tests was taken to correspond with the gas pressure at which water outflow was first detected at the upper face of the specimen. It was therefore assumed that an outflow of water signified an inflow of gas. Threshold pressures were in the range 10 to 60 kPa, which is very low when compared with those of bentonite with no sand addition.

2.1 Experiments on Fo-Ca clay and Kunigel VI bentonite

/Gallé, 1998/ described a programme of gas migration experiments on Fo-Ca clay, which is the French candidate material for the construction of clay barriers. This clay comes from the Vexin region of France (Fourges-Cahaignes) in the west of the Paris Basin. The clay is essentially a calcium smectite with interstratified kaolinite-beidellite as a primary constituent, together with some quartz, goethite and calcite. When compacted to a dry density of 1.75 $Mg.m^{-3}$, the clay has an intrinsic permeability (to water) of around 5 x 10^{-21} m^2 and a swelling pressure of around 14 MPa.

Hydrogen migration experiments were conducted using a high-capacity oedometer. The equipment allowed for a maximum gas inlet pressure of 9.3 MPa cell /Gallé, 1995; Tanai et al, 1997/. The clay specimens were 50 mm in diameter and 40 mm high. The samples were prepared by compacting pre-conditioned Fo-Ca clay powders in the cell to dry densities of 1.60, 1.70, 1.80 and 1.90 $Mg.m^{-3}$ under a uniaxially-applied stress. These dry densities correspond to porosities of 0.4, 0.36, 0.32 and 0.29, respectively. Each batch of powder was pre-conditioned in water vapour at a fixed relative vapour pressure by storing it for a period of several months in a closed vessel. Vapour pressures were held constant using salt solutions. In order to examine the behaviour of saturated clay, a number of the specimens were backpressured with water at a pressure larger than atmospheric pressure.

The test involved raising the gas pressure on one end of the specimen in small steps. Increments of 0.1 to 0.05 MPa were applied for periods of 12 to 24 hours. The specimen was not actively stressed at its boundaries and water pressure was not applied to the downstream end of the specimen. When gas outflow was observed at the downstream end, the flow rate was measured to determine gas permeability. Gas pressure was then raised. Permeability was calculated using the Hagen-Poiseuille relationship.

/Gallé, 1998/ observed two distinct thresholds. The gas pressure at the lower threshold was termed the gas entry pressure, and coincided with the first appearance of gas at the downstream end of the specimen. The upper threshold was characterised by a sharp increase in measured flow rate. The term breakthrough pressure was applied to the critical gas pressure at the upper threshold. Breakthrough pressure was always larger than the gas entry pressure, although these two thresholds were found to be very close in the fully saturated clay. The gas permeability of Fo-Ca clay was found to decrease systematically with increasing degree of saturation and with increasing dry density (Table 2-1). For clay specimens with fixed dry density and varying degrees of saturation in the range 70 to 100%, gas permeability was found to vary by three orders of magnitude. For specimens with a fixed degree of saturation, an increase in dry density of only 0.1 $Mg.m^{-3}$ was found to decrease gas permeability by an order of magnitude.

/Tanai et al, 1997/ measured the gas permeability of Kunigel VI as a function of saturation. The specimens were made by uniaxial compaction of pre-conditioned clay powders in the oedometer-type test vessel. Specimens were 50 mm in diameter and 10 mm thick. Dry densities were 1.6, 1.7 and 1.8 $Mg.m^{-3}$. Pre-conditioning involved: (a) oven-drying at 110ºC for 24 hours so as to achieve zero water content; (b) air-drying to achieve a gravimetric water content less than 9%; and (c) spraying with a fine mist of water to achieve a water content greater than 9%. Gas permeability at a degree of saturation of zero (i.e. no water) was taken as a measure of the intrinsic permeability of the clay. Values were around 1 x 10^{-15} m^2. Intrinsic permeabilities measured on saturated material using water as a permeant were around five order of magnitude

Table 2-1. Variation of the hydrogen gas effective permeability (m^2) with dry density and degree of saturation for Fo-Ca clay /from Gallé, 1998/. Degree of saturation refers to the state of the specimen before gas entry.

Degree of saturation, S_r (%)	Dry density ($Mg.m^{-3}$)			
	1.60	1.70	1.80	1.90
74	$1.7\pm0.3 \times 10^{-16}$	$2.8\pm0.7 \times 10^{-17}$	$5.8\pm1.4 \times 10^{-18}$	$3.1\pm0.5 \times 10^{-19}$
82	–	$9.2\pm2.6 \times 10^{-18}$	$3.4\pm0.7 \times 10^{-18}$	$2.7\pm0.4 \times 10^{-20}$
90	–	$1.7\pm0.6 \times 10^{-18}$	$1.5\pm0.1 \times 10^{-19}$	–
97	$3.9\pm2.4 \times 10^{-18}$	–	$5.1\pm1.5 \times 10^{-20}$	–
100	$1.1\pm0.1 \times 10^{-18}$	2.0×10^{-19}	4.5×10^{-20}	2.5×10^{-22}

smaller than those established using gas. The researchers tested the applicability of three saturation functions, the Corey model, the Fatt and Klikoff model and the Sandia model. The Corey model provided the best fit to the data. The relative permeability to gas of Kunigel VI approaches zero at a degree of saturation of around 72%. This marks the saturation at which there are no continuous gas channels through the bentonite and breakthrough pressure therefore becomes finite.

/Tanai et al, 1997/ also examined the relationship between the dry density, the swelling pressure and the breakthrough pressure of saturated Kunigel VI and French Fo-Ca clay. Clay powder was compacted uniaxially to a target dry density in the oedometer cell and then water at fixed head was supplied to the lower porous disc. Hydrogen was used for the gas migration experiments. An initial gas pressure of 0.5 MPa was applied to the lower surface of the specimen. Gas pressure was raised in increments of 0.5 MPa, applied at time intervals of 120 hours. Breakthrough pressures were close to the measured swelling pressures for both clay-types.

2.2 Experiments on Canadian Avonlea bentonite

/Hume, 1999/ reported a detailed laboratory study on compacted Avonlea (or Saskatchewan) bentonite. The first series of experiments used a constant volume cell described in detail by /Kirkham, 1995; Gray et al, 1996/. An initial gas pressure differential of 0.2 MPa was applied to the clay plugs and this pressure was increased by 0.2 MPa every 5 minutes to a maximum of 10 MPa. Tests on unsaturated plugs showed the breakthrough pressure to be negligible below a degree of saturation of around 80 to 90%. Breakthrough pressures were found to increase very rapidly as saturation approached 100%, in some cases exceeding the 10 MPa capacity of the apparatus.

Given the large breakthrough pressure of dense Avonlea bentonite close to full saturation, a second constant volume apparatus was constructed with a pressure rating of 50 MPa. A gas pressure differential of 0.8 MPa was applied to the plugs at the onset of a test and this was increased by 1.0 MPa every 5 minutes until the limit of the apparatus was reached. Although it was feasible to obtain breakthrough for dry densities greater than 1.15 $Mg.m^{-3}$ using this apparatus, it was discovered that the wetting

procedure was not producing complete saturation of the clay. When the wetting procedure was improved by applying 5 MPa of water pressure to the specimens for a period of 2 days, consistent gas breakthrough could not be obtained for dry densities greater than 0.6 $Mg.m^{-3}$.

Tests were also conducted on saturated specimens at constant gas pressure. Breakthrough pressures were in the range 0.3 to 19.8 MPa for dry densities in the range 0.8 to 1.4 $Mg.m^{-3}$. Breakthrough occurred in all of these tests, but often after a much longer period of time than the typical duration of the increasing pressure tests. At a dry density of 1.0 $Mg.m^{-3}$ (breakthrough pressures in the range 0.8 to 1.4 MPa), an inverse relationship was found between the time to breakthrough and the breakthrough pressure.

Hume's opinion was that the time to breakthrough was likely to be determined by the time required for water to flow from the specimen so as to create a passage for gas. The postulated inverse relationship implies that the breakthrough pressure would be zero for an infinitely large testing period. This would, of course, deny the existence of a finite capillary entry pressure governing the flow of gas into a saturated porous medium with very narrow pores. /Hume, 1999/ does however make the comment that the Canadian constant pressure gas test results "do not exclude the possibility of a capillary threshold pressure for gas entry".

2.3 Experiments on saturated clay pastes

/Donohew et al, 2000/ described a programme of simple gas injection experiments on unconfined and initially water-saturated clay pastes at water contents between the liquid and plastic limits. The aim was to investigate the relationships between gas entry pressure, water content and plasticity for a range of clay types, to define the principal mechanisms of gas entry and flow by simple visual observations, and to determine the effects of previous gas injection and residual gas content on entry pressure.

By examining entry mechanisms across the full range of water contents, it was possible to delineate three basic modes of behaviour. Mechanism BB, or gas movement in buoyant bubbles and cavities, is common to most clays at high to intermediate water contents and is associated with relatively low gas entry pressures (<100 kPa). Mechanism TFR, or gas movement in tension fractures with rapid and complete loss of gas pressure, occurs in all clays at low water contents and gives high gas entry pressures (>100 kPa). Mechanism TFG is characterised by tension fractures exhibiting slow propagation and a gradual loss in internal gas pressure. It occurs at intermediate water contents and can be interpreted as transitional between mechanisms TFR and BB.

There was no evidence in any of these tests that gas actually penetrated or flowed through the intergranular porosity of the clay matrix. In all cases, gas made its own volume by pushing back the paste and lifting the free surface of the sample. Gas entry at high pressures in this clay was audible and occasionally violent. After gas injection, remnant gas-filled voids and cracks remained within the clay. These were re-opened during repeated injections at pressures which were only a fraction of the entry pressures of the gas-free pastes.

Gas entry pressures in the region of the plastic limit were surprisingly large, particularly for clay types with high total specific surface and plasticity index. /Fleureau et al, 1993/ found a correlation between the air entry value (*AEV*) of a clay soil and its liquid limit.

The *AEV* can be broadly equated with the excess gas pressure relative to porewater pressure necessary to obtain gas entry. For soils with 60% or more particles smaller than 80 μm, the *AEV* can be predicted using the linear relationship

$$AEV = 32.4 w_L - 466.7 \quad \text{(kPa)} \qquad 2\text{-}1$$

where w_L is the liquid limit expressed as a percentage. The correlation coefficient for this relationship, r^2, was found to be 0.84. Since the liquid limit of Mx-80 bentonite is around 330%, this empirical relationship predicts an air entry value for saturated buffer bentonite of around 10.2 MPa. The existence of a finite and large capillary threshold pressure for gas entry in bentonite is therefore demonstrable on the basis of known trends in material behaviour.

2.4 Experiments on saturated Mx-80 bentonite under isotropic stress conditions

/Horseman et al, 1997, 1999/ and /Harrington and Horseman, 1999/ reported a series of controlled flow rate gas injection experiments on pre-compacted Mx-80 buffer bentonite. Specimens were fully saturated (>99%) and equilibrated under confining stress with an external water pressure (i.e. backpressure) of 1.0 MPa applied at both ends. Net flows were monitored to establish the point of equilibration. Helium was used as a permeant. Gas was injected at constant flow rate. Four experiments provided data amenable to quantitative interpretation. Gas permeability, k_g (m^2), was calculated using the following relationship for the laminar flow of a compressible gas

$$Q_{st} = \frac{v_{mst} k_g A_s}{2 \mu_g L_s RT} \left[(p_{gi})^2 - (p_{wo} + p_{co})^2 \right] \qquad 2\text{-}2$$

where Q_{st} ($m^3.s^{-1}$) is the post-breakthrough volumetric flux of gas at standard temperature and pressure (STP), v_{mst} ($m^3.mol^{-1}$) is the molar volume of the gas at STP, μ_g (Pa.s) is the dynamic viscosity of the gas, R ($J.mol^{-1}.K^{-1}$) is the gas constant, T (K) is the absolute temperature, p_{gi} (Pa) is the upstream gas pressure, p_{wo} (Pa) is the downstream water pressure, and A_s (m^2) and L_s (m) are the cross-sectional area and length respectively of the test specimen. Parameter p_{co} (Pa) was termed the apparent capillary pressure and defined as the pressure difference between gas and water at the downstream end of the specimen. Permeability values calculated in this way are somewhat model dependent.

Test history Mx80-4 on bentonite with dry density of 1.67 $Mg.m^{-3}$ is representative of these experimental findings. Figure 2-1 shows the first stage of this history, where confining stress and backpressure were 16.0 and 1.0 MPa, respectively. An initial pumping rate of 375 $\mu l.hr^{-1}$ was used to raise the upstream gas pressure. Gas breakthrough occurs at an excess pressure (relative to backpressure) of 15.2 MPa, which is fractionally larger than the calculated swelling pressure of the clay, confirming the findings of others on the importance of swelling pressure in the gas migration process in initially saturated buffer clays /Pusch et al, 1985; Tanai et al, 1997/.

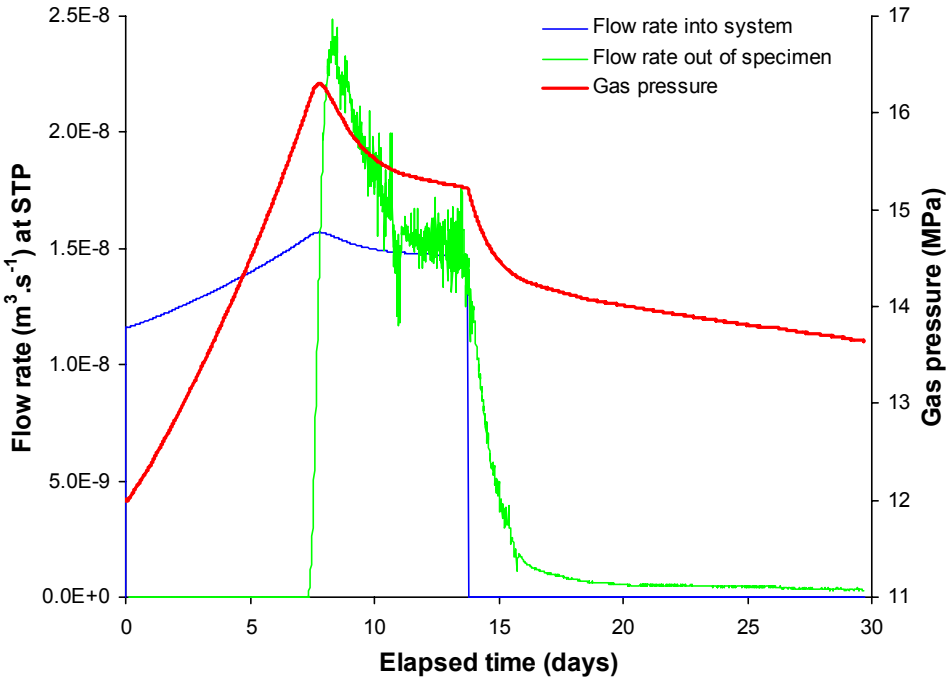

Figure 2-1. *Gas pressure and volumetric flow rates (STP) into the testing system and out of the specimen plotted against elapsed time. The material is HS-batch (high swelling) clay with an average dry density of 1.64 Mg.m^{-3} and a swelling pressure close to 15 MPa. The peak pressure response is suggestive of the propagation of gas-conductive pathways.*

The peak pressure, at 16.3 MPa, is probably indicative of some sort of fracturing process and is followed by a spontaneous and very well-defined negative transient which approaches an asymptotic value of 15.2 MPa.

The gas injection pump was then stopped so as to determine the 'shut-in' transient. The extrapolated asymptote of the transient, plotted as excess gas pressure (relative to backpressure) against time, is the apparent capillary pressure, p_{co}, of Equation 2-2.

Gas injection was reinstated at the same pumping rate. Figure 2-2 shows no well-defined breakthrough event and gas flow through the specimen commences at an excess pressure substantially lower than that of the fresh specimen. Pressure climbs to a rather inconspicuous secondary peak at 15.3 MPa. The possible explanation for the lack of a distinctive breakthrough event and the substantial reduction in the peak excess pressure is that the gas pathways in the bentonite failed to close up completely during the preceding shut-in stage.

The specimen was then subjected to a descending history of pumping rates (180, 90, 45 and 0 μl.hr^{-1}). Each stage gave the characteristic negative transient. As a rough rule of thumb, halving the gas flow rate at each stage leads to more or less equal decrements in the steady-state gas pressure. The gas flow law is therefore nonlinear (i.e. non-Darcian), leading to a variable gas permeability. The very substantial duration of the shut-in response is a direct consequence of this underlying nonlinearity. Gas pressure fell to 12.6 MPa after 24 days.

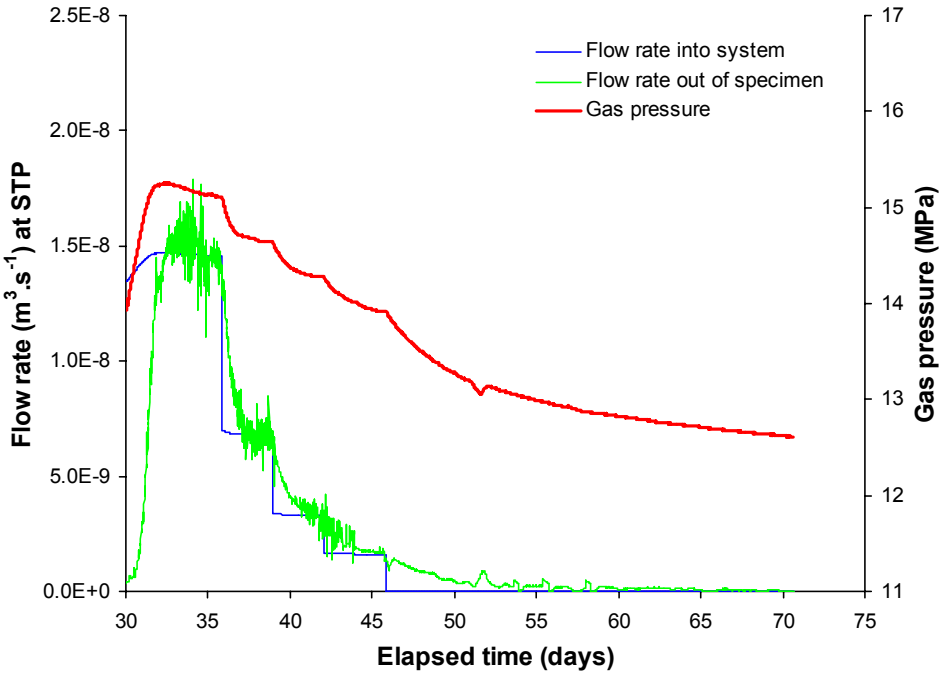

Figure 2-2. *Gas pressure and volumetric flow rates (STP) into the testing system and out of the specimen plotted against elapsed time for the same specimen as in Figure 2-1, but restarted after the period of shut-in. The peak is substantially lower than for the fresh clay suggesting that gas pathways formed in the first cycle were not fully closed at the onset of the second testing cycle.*

Although the gas permeabilities were clearly flow-rate dependent, they varied over quite a narrow range. Under 16.0 MPa confining pressure and 1.0 MPa back-pressure, clay with a dry density of 1.68 $Mg.m^{-3}$ gave gas permeabilities in the range 1.7 to 2.7 x 10^{-20} m^2 at the specified flow rate. Under 8.0 (and 9.0) MPa confining pressure and 1.0 MPa backpressure, clay with a dry density of 1.58 $Mg.m^{-3}$ gave gas permeabilities in the range 1.7 to 2.2 x 10^{-20} m^2 at the same flow rate. These values can be compared with intrinsic permeabilities (for water), estimated from published data, of around 0.6 x 10^{-20} m^2 and 1.1 x 10^{-20} m^2 for the high and low density clay, respectively. Given the very low gas contents of the bentonite specimens after gas injection, the measured gas permeabilities cannot be reconciled with the intrinsic permeabilities by invoking physically reasonable values for the relative permeability to gas.

/Horseman and Harrington, 1997/ suggested that gas does not flow through the original pore space of water-saturated bentonite. In their view, the measured gas permeability from these tests is a dependent variable rather than a material property, since it depends on the number of pressure-induced pathways linking gas source to sink, together with the width and aperture distributions of these features.

Conclusive evidence of gas penetration of test specimens was obtained by immersing previously gas-tested bentonite in a beaker of glycerol and gently heating so as to expand and release helium trapped along the flow pathways. Streams of gas bubbles were observed emerging at numerous discrete points on all surfaces of the clay. Since

helium solubility in clay porewater is extremely low, this suggests that gas moved through the clay as a discrete phase, following multiple pathways. No emergent gas bubbles were observed in a control experiment on fresh bentonite /Harrington and Horseman, 1999/.

One specimen in this test programme contained a fabrication joint which, in effect, divided the specimen into two half-cylinders. This test was intended to simulate the effect, if any, of a joint between individual buffer clay blocks. Comparison with a specimen with no joint showed that the block fabrication joint had no discernible effect on the gas transport properties of the fully hydrated buffer clay.

2.5 Outstanding issues

Tests on unsaturated Avonlea bentonite have shown breakthrough pressure to be negligible below a degree of saturation of around 80 to 90% /Hume, 1999/. This range marks the saturation at which there are no continuous gas channels through the clay. In Kunigel VI bentonite, the critical saturation for interconnected gas voids was found to be 72% /Tanai et al, 1997/. Breakthrough pressures were found to increase very rapidly as saturation approached 100% /Hume, 1999/. Although there is some disagreement between experimentalists on the question of gas pressurisation rate, there is evidence to suggest that the threshold pressure for gas entry into initially-saturated bentonite at typical buffer dry densities is of large magnitude /Pusch et al, 1985; Pusch et al, 1987; Tanai et al, 1997; Horseman et al, 1997, 1999; Harrington and Horseman, 1999/.

All controlled flow rate experiments on saturated clay showed a peak in gas pressure, followed by a spontaneous negative transient /Horseman et al, 1997, 1999/. The peak is similar to that observed during hydrofracturing, suggesting that gas moves as a discrete phase through a network of interconnected cracks formed by tensile (or possibly extensile) rupture of the clay /Harrington and Horseman, 1999/. /Rodwell et al, 1999/ noted that the height of the pressure peak might be sensitive to the rate of gas injection.

/Pusch and Forsberg, 1983/ found that the degree of saturation of specimens after passage of the gas through Mx-80 was very close to 100%, suggesting that the gas must have passed through a small number of discrete pathways causing minimal desaturation of the pores. Experiments reported by /Donohew et al, 2000/ suggest that a saturated clay must dilate (that is, grow in volume) during gas entry and the initial changes in gas content are accommodated by an increase in the total volume of the clay. Although this is consistent with gas flow through a network of pressure-induced pathways, it cannot be reconciled with the more usual soil mechanics concept of desaturation by direct displacement of porewater. If all gas in the clay is accommodated by dilatancy, this raises the important question of sensitivity of the gas transport process to the boundary conditions of an experiment /Horseman et al, 1999/. Since the buffer clay will be confined between the non-yielding surfaces of the metal waste canister and the semi-rigid walls of the emplacement borehole, the key question arises – will the breakthrough behaviour be the same if the bentonite is not allowed to change its volume during gas injection?

Focussing on issues that are important to repository performance assessment, two main questions arise. The first is whether it is possible for gas generated inside a canister to displace porewater from the buffer clay. The second is whether the passage of gas through the buffer can in any way compromise the sealing capacity of the clay. Two mechanisms can be postulated by which gas at high pressure might drive water out of the buffer. Conventional two-phase flow theory would suggest that gas movement into a clay must be accompanied by the drainage of water from the pore space. Alternatively, gas at high pressure might exert a total stress on the clay fabric, tending to consolidate and de-water the clay mass. This is an indirect mechanism of porewater expulsion and is quite distinct from the displacement mechanism. It can be surmised that high excess gas pressures would be necessary to cause buffer consolidation. Given the evidence for pathway flow of gas in buffer, the resealing of the gas migration pathways after the passage of the gas is an important consideration in assessing the long-term performance of the buffer.

3 Experimental methodology

Two test geometries were used in this study to examine the role of the boundary stress and its effect on gas penetration and subsequent movement through initially saturated buffer clay material.

3.1 Constant volume and radial flow (CVRF) geometry

In this test geometry (tests Mx80-8 and Mx80-10), the specimen is volumetrically constrained, preventing dilation of the clay in any direction. This BGS custom-designed apparatus, named the constant volume and radial flow (CVRF) permeameter (Figure 3-1), has six main components: (1) a thick-walled, dual-closure stainless steel pressure vessel; (2) an injection pressure system; (3) three independent backpressure systems; (4) five total stress gauges[1] to measure radial and axial total stresses; (5) a porewater pressure monitoring system; and (6) a microcomputer-based data acquisition system.

The pressure vessel comprises a dual-closure tubular vessel manufactured from 316 stainless steel and pressure-tested at 69 MPa. Each of the end-closures is secured by twelve high tensile cap screws which can also be used to apply a small pre-stress to the specimen if required.

The 60 mm internal bore of the pressure vessel is honed to give a highly polished surface. All ports, except those for the direct measurement of stress, contain sintered stainless steel porous plugs which are profiled to match the bore of the pressure vessel. The stress gauges are an in-house design which uses a 6.4 mm steel push-rod fitted with an ‘O’-ring seal to compress a small volume of liquid contained in a chamber at the front face of a miniature Sensotec Model PX600-3KGV pressure transducer. In the porewater pressure sensor, the push-rod is replaced by a sintered stainless steel porous plug enabling water pressure to act on the front face of the transducer. The layout of the stress and pressure sensors is shown in Figure 3-1.

The central or ‘source' filter is embedded at the end of a 6.4 mm diameter stainless steel tube and is used to inject the permeant, either helium or distilled water. The end of the filter is profiled to match a standard twist drill. A 1.6 mm diameter tube passes down the bore of the filter tube to enable flushing of the tube prior to gas injection.

Figure 3-2 shows a photograph of the injection end-cap, sintered stainless steel injection port, axial stress device and the large stainless steel drainage filter. Also visible is the small stainless steel push-rod which transmits the boundary stress, via a sealed reservoir filled with an incompressible fluid, to a miniature flat-face pressure transducer.

[1] Only two stress sensors were used in Mx80-8, with three more added prior to Mx80-10.

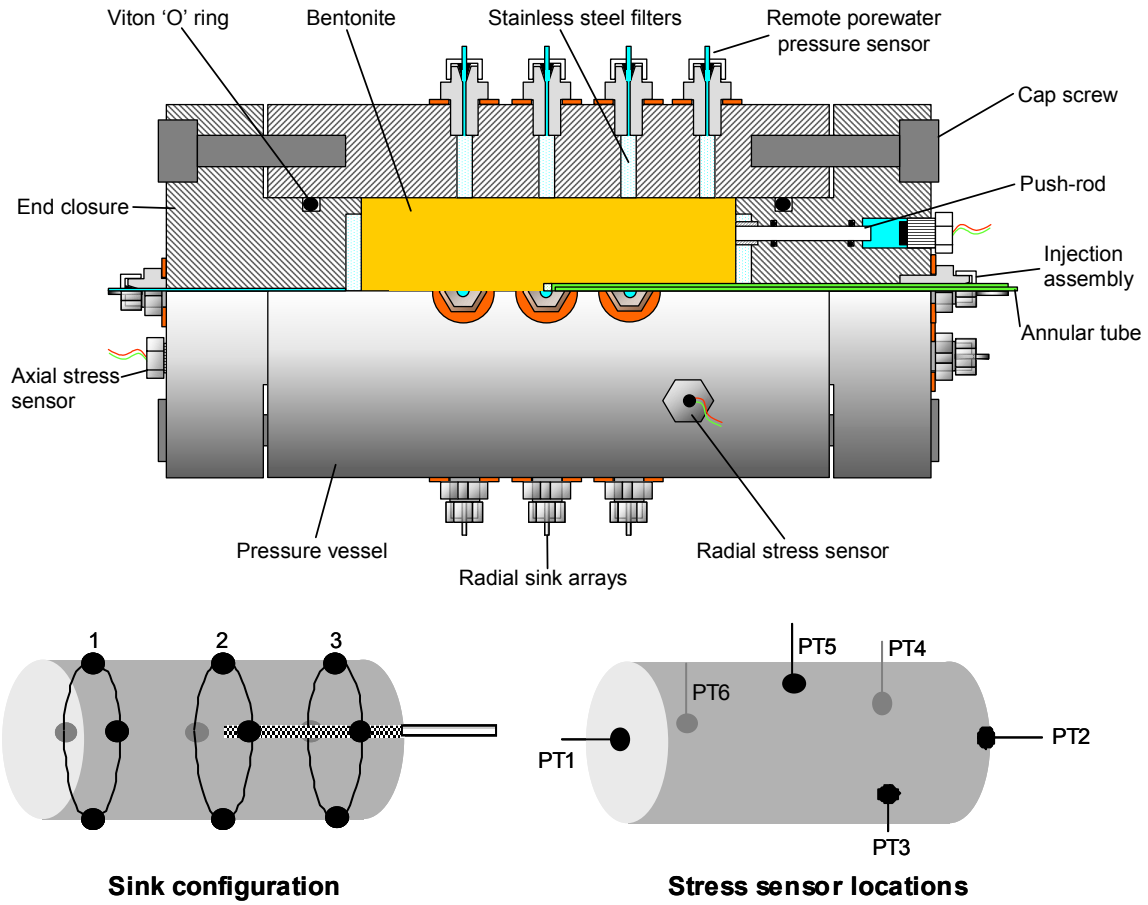

Figure 3-1. *Cut-away diagram of the constant volume and radial flow (CVRF) gas migration apparatus. Sensors are as follows: [PT1] – axial total stress on the backpressure end-closure, [PT2] – axial total stress on the injection end-closure, [PT3] – radial total stress close to the injection end-closure, [PT4] – porewater pressure close to the injection end-closure, [PT5] – radial total stress at the mid-plane, and [PT6] – radial total stress close to the backpressure end-closure.*

Pressure and flow rate of test fluids are controlled using four ISCO-500, Series D, syringe pumps, operating from two independent control units. Given the potential for gas leakage past the injection pump seal, a constant flow rate is developed by displacingthe gas from a pre-charged Whitey cylinder. This helps to ensure that the helium is water-saturated prior to injection, reducing the potential for desiccation. The ISCO pump controllers have an RS232 serial port, which allows volume, flow rate and pressure data from each pump to be transmitted to an equivalent port on a 32-bit personal computer. Additional test parameters are logged using an A/D converter card fitted to the computer. Typical acquisition rate is one scan per fifteen minutes.

For the tests conducted as part of this study, all the sensors were calibrated against laboratory standards by applying incremental steps in pressure, from atmospheric to a pre-determined maximum value. This was followed by a descending history to quantify any hysteresis. Least-squares fits were calculated and the regression parameters used to correct raw data.

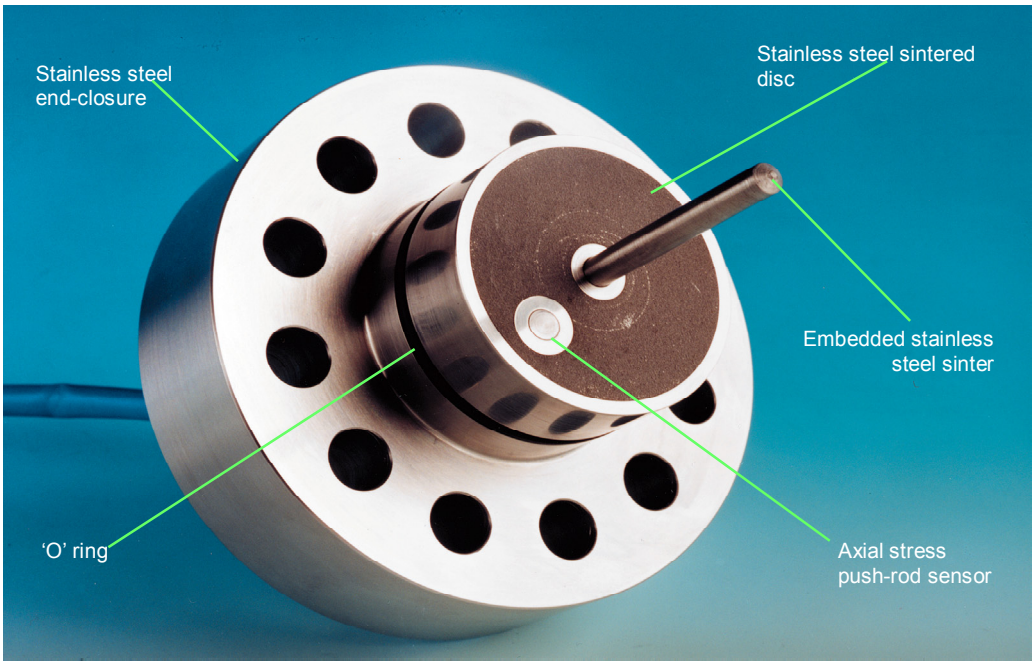

Figure 3-2. *Injection end-closure showing stainless steel sintered drainage disc, axial stress push-rod sensor, Viton 'O' ring and embedded injection filter.*

In test Mx80-8 the stress sensors failed to respond to the increase in total stress during the swelling and hydration phase but showed clear responses to elevated gas pressure. A number of design modifications were made prior to test Mx80-10 and it is clear that the sensors were fully functional during this second CVRF test.

3.2 Radially-constrained K_0 apparatus

In this geometry (test Mx80-9), the specimen is radially constrained, with strain only possible in the axial direction. The Teflon sheath, commonly used in isotropic tests /Horseman and Harrington, 1997/, is replaced by a thick-walled stainless steel sleeve (Figure 3-3). Axial stress on the specimen is developed by two pistons which are free to move within the steel sleeve. The pistons are pressed onto the clay by the confining fluid and therefore transmit confining pressure to the ends of the specimen. Since lateral strain is prevented, the stress state of the specimen is essentially that of a K_0-type soil test /Lambe and Whitman, 1969/. Each piston has an 'O'-ring seal and two ports to allow the interchange of fluid phases during the course of the experimental history.

The thick-walled sleeve is designed to allow porewater pressure to be measured at a point equidistant from the upstream and downstream faces of the cylindrical specimen. A 6.4mm diameter stainless steel sinter is flush-mounted inside the steel sleeve and connected to a remote pressure transducer by small-bore nickel tubing.

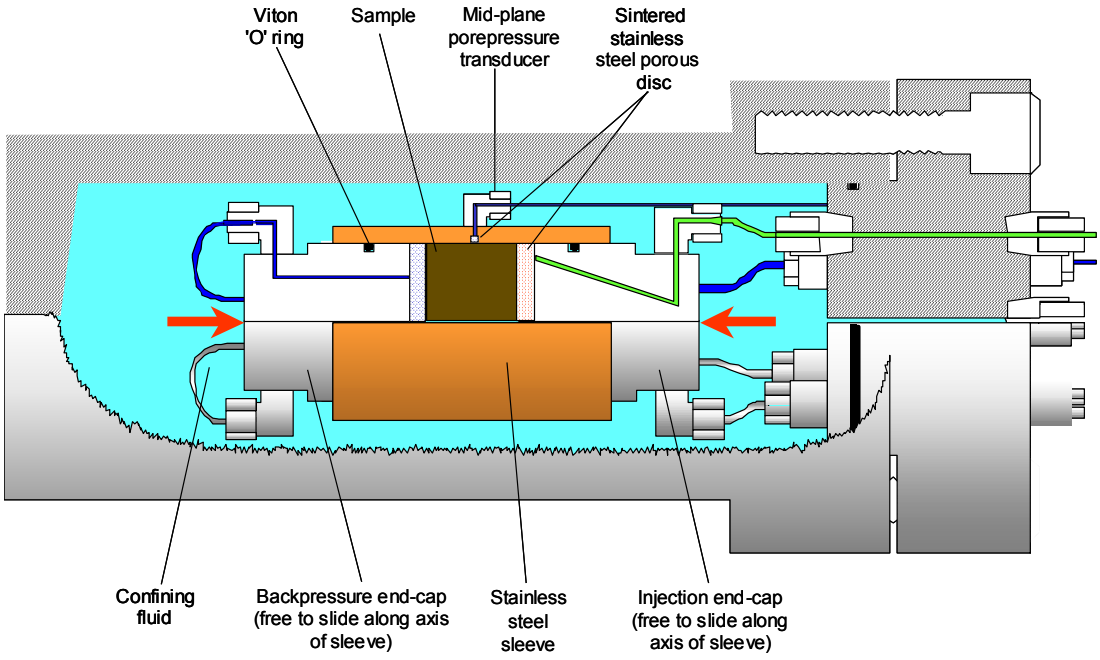

Figure 3-3. *Schematic diagram of the pressure vessel and sample assembly for the radially-constrained K_0 apparatus.*

3.3 Specimen preparation and dimensions

Pre-compacted bentonite blocks were manufactured by Clay Technology AB (Lund, Sweden) by rapidly compacting Mx-80 bentonite granules in a mould under a one-dimensionally applied stress /Johannesson et al, 1995/. On receipt at BGS Keyworth, the preserved blocks were stored in a refrigerator prior to specimen preparation. Test specimens were manufactured by hand-trimming using a tubular former with a sharpened leading edge. The upper and lower surfaces were finished using a scraping action with a flat-bladed knife, leaving the end surfaces flat and parallel. The dimensions and orientation of each test specimen with respect to the axis of compression during block fabrication are given in Table 3-1.

In the CVRF tests, the specimen preparation former was mounted in a lathe and a 6.4 mm diameter hole drilled in the clay to accommodate the source filter and tubing assembly (Figure 3-3). The specimen was then extruded from the former into the pressure vessel using a screw-driven press.

3.4 Physical properties

Table 3-2 shows the basic physical properties of each test specimen. Water content was determined by oven-drying at 105°C for a period in excess of 24 hours. Void ratio, porosity and degree of saturation are based on an average grain density for the bentonite of 2.77 $Mg.m^{-3}$.

Table 3-1. Specimen details.

Specimen number	Test type	Orientation to compression axis	Diameter (mm)	Length (mm)	Pre-test volume (ml)
Mx80-8	CVRF	Perpendicular	60	120	337.6
Mx80-9	K0	Perpendicular	51	51	103.6
Mx80-10	CVRF	Perpendicular	60	120	337.6

Table 3-2. Basic physical properties of the test specimens.

Specimen number	Block number	Water content (wt %)	Bulk density ($Mg.m^{-3}$)	Dry density ($Mg.m^{-3}$)	Void ratio	Initial saturation (%)
Mx80-8	BGS4	26.7	1.997	1.577	0.756	97.6
Mx80-9	BGS4	27.1	1.993	1.568	0.767	98.0
Mx80-10	BGS99	26.7	2.005	1.582	0.751	98.6

4 Results

4.1 Buffer hydration

All specimens were fully-hydrated before gas testing by backpressuring using de-aired and distilled water. This procedure gave initial degrees of saturation which were demonstrably close to 100%. The instrumentation of test Mx80-10 enabled the development of swelling pressure and the variation of total stress with the applied backpressure to be studied.

4.1.1 Development of swelling pressure

Swelling pressure was measured in test Mx80-10. The specimen was exposed to de-aired and distilled water at a backpressure of 1.0 MPa which was applied to all filters. Figure 4-1 shows the increase in the total stress as swelling pressure develops over time. The fluctuations in stress between two and seven days are caused by temperature changes in the environmental chamber associated with temporary problems with the air-conditioner.

At equilibrium, the total stress registered by the sensors varies from 6.6 MPa, close to the backpressure end of the specimen, to 6.0 MPa at the mid-point of the specimen. The average total stress acting on the five sensors is 6.4 MPa. For a clay-water system with the porewater in thermodynamic equilibrium with an external reservoir of water at pressure, p_w, the total stress acting on the surrounding vessel can be expressed as

$$\sigma = \Pi + \alpha\, p_w \qquad 4\text{-}1$$

where Π is the swelling pressure and α is a proportionality constant /Harrington et al, 2002/. Taking $\alpha = 0.86$ (see below) and $p_w = 1.0$ MPa gives a swelling pressure of 5.5 MPa.

4.1.2 Sensitivity of total stress to changes in backpressure

The sensitivity of total stress to changes in the externally-applied water pressure was examined in test Mx80-10. Backpressure was incremented in 1.0 MPa steps to a maximum value of 7.0 MPa, and then lowered to 4.0 MPa and finally back to 1.0 MPa. The total stress and porewater pressure sensors were continually monitored (Figure 4-2). Data are presented in Table 4-1. As the externally-applied water pressure increases, the total stress acting on the specimen becomes progressively more homogeneous. At the lowest backpressure value of 1.0 MPa, the variation in total stress across the specimen is around 0.6 MPa.

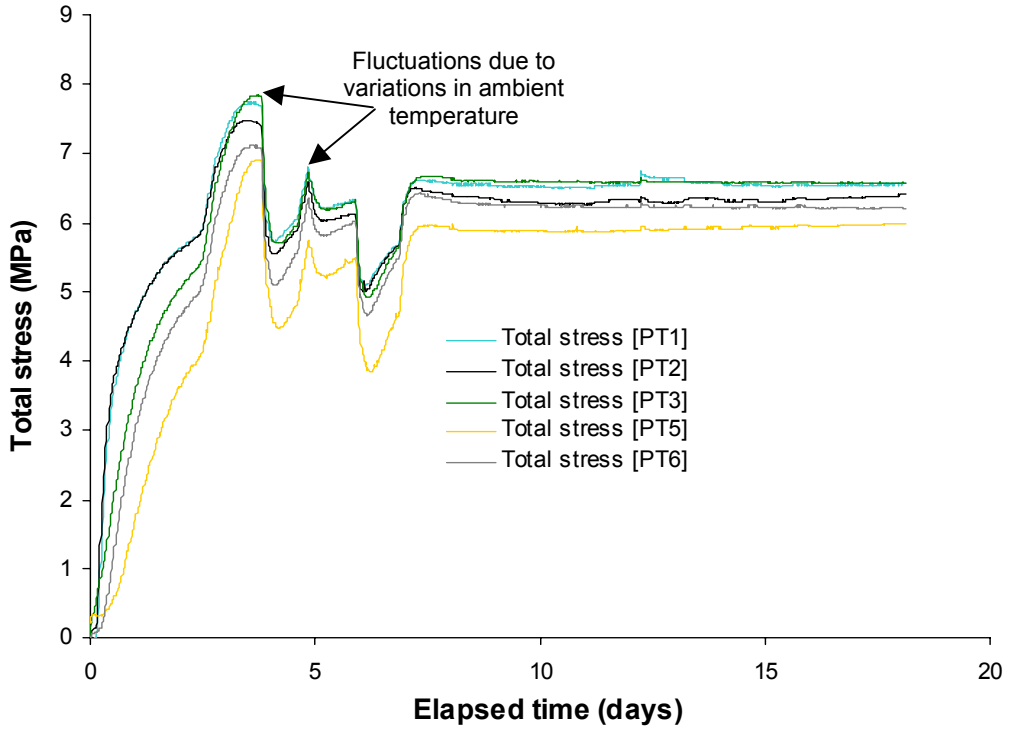

Figure 4-1. *Initial hydration stage of test Mx80-10 showing the increase in total stress as swelling pressure develops over time. The fluctuations are caused by temperature changes in the environmental chamber associated with temporary problems with the air-conditioner.*

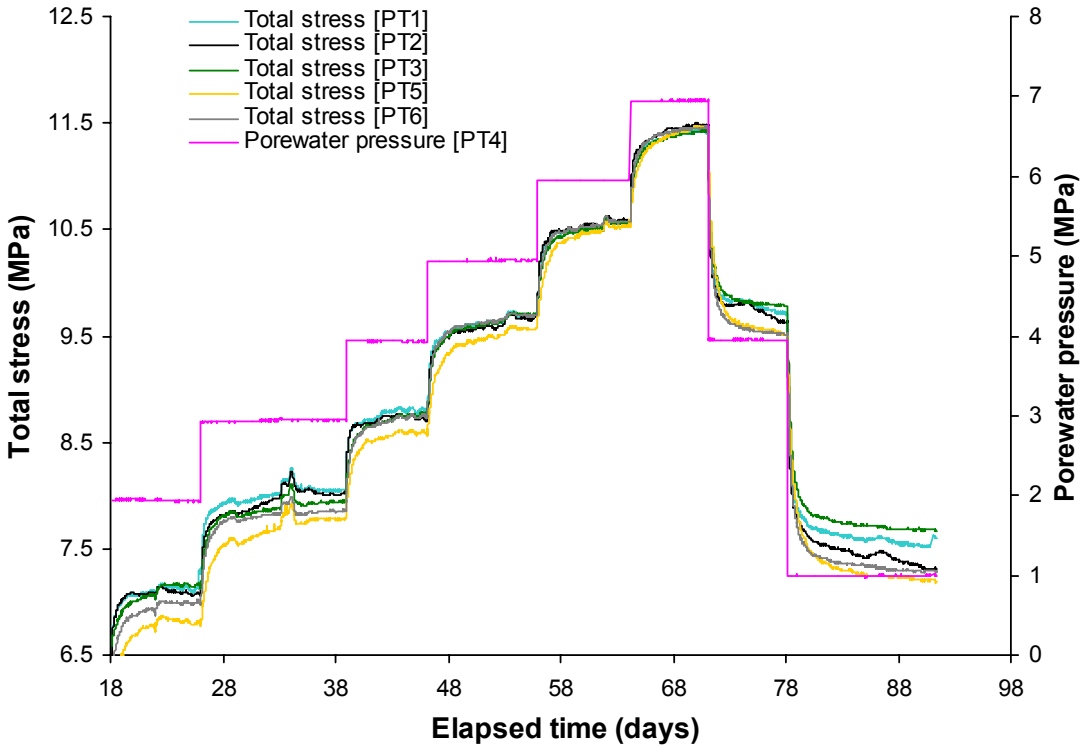

Figure 4-2. *Monitored changes in total stress on specimen Mx80-10 as the external porewater pressure (backpressure) is incremented and decremented.*

Table 4-1. Axial and radial total stresses over a history of varying backpressure.

Back-Pressure (MPa)	Total stress (MPa)					
	Axial backpressure end-cap [PT1]	Axial injection end-cap [PT2]	Radial injection end [PT3]	Radial middle [PT5]	Radial backpressure end [PT6]	Average
1.0	6.56	6.41	6.57	5.98	6.21	**6.35**
2.0	7.27	7.07	7.12	6.76	6.97	**7.04**
3.0	8.06	8.02	7.94	7.79	7.86	**7.93**
4.0	8.77	8.70	8.75	8.57	8.73	**8.70**
5.0	9.71	9.70	9.71	9.57	9.69	**9.68**
6.0	10.56	10.58	10.56	10.53	10.57	**10.56**
7.0	11.42	11.48	11.44	11.48	11.46	**11.46**
4.0	9.72	9.64	9.78	9.50	9.51	**9.63**
1.0	7.59	7.31	7.67	7.19	7.29	**7.41**

At the highest backpressure value of 7.0 MPa, this difference decreases to under 0.1 MPa. This behaviour might be linked to residual air bubbles moving into solution as the backpressure increases or to changes in side-wall friction as total stress increases. The very slow rise in stress on the mid-plane radial stress sensor [PT5] also suggests that there may be a time lag in achieving full hydration in parts of the clay remote from the filters used for backpressuring.

Figure 4-3 shows a plot of the average total stress against the applied backpressure. Linear regression of the equilibrium stresses gives α = 0.86 for the incremental history. Extrapolation of the best fit line to the intercept at zero backpressure gives Π = 5.4 MPa, which is slightly smaller than the value measured during hydration. Hysteresis is evident in the decremental history, with α = 0.74 and an intercept of 6.7 MPa. Possible reasons for $\alpha \neq 1$ and for the hysteretic behaviour include side-wall friction between the clay and the steel vessel, the presence of residual air bubbles in the clay and the finite compliance of the sensors used to measure the total stress.

4.2 Permeability to water

The hydraulic permeability of Mx80 buffer bentonite was examined using the two experimental geometries. In the first tests (Mx80-8 and Mx80-10) the specimen was volumetrically constrained and prevented from swelling in all directions by the body of the pressure vessel (see section 3.1). In the second test (Mx80-9) the specimen was radially constrained but free to swell in an axial direction.

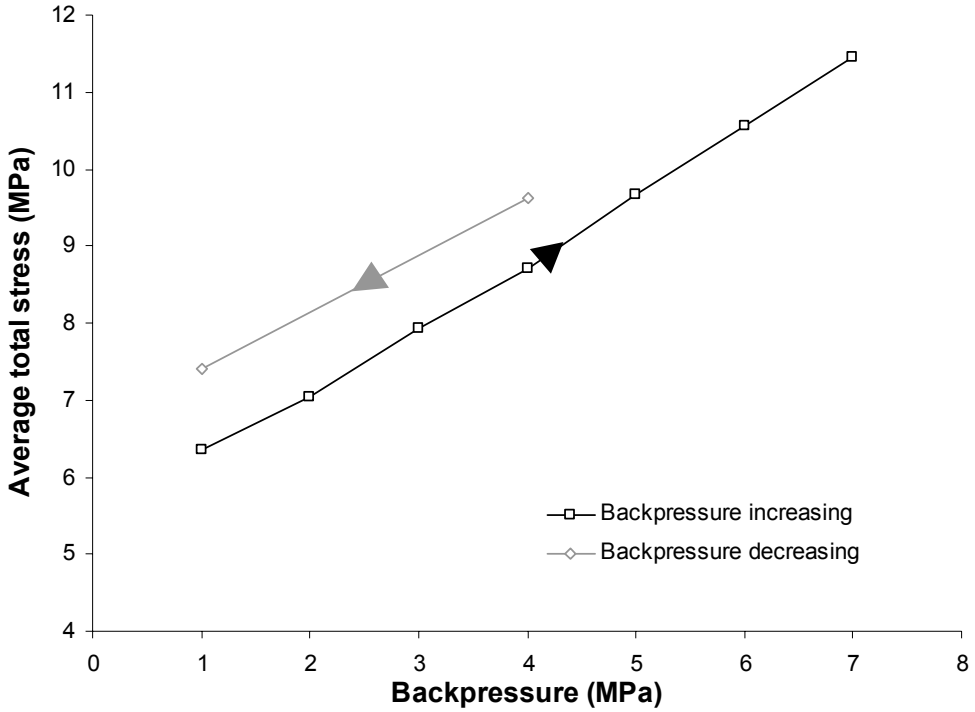

Figure 4-3. *Average total stress plotted against externally-applied water pressure (backpressure). The data are presented in Table 4-1.*

4.2.1 Permeability under constant volume conditions

To determine the permeability to water of specimen Mx80-8, a sequence of constant pressure gradient test stages were performed with the flow of water from the central source filter to the radial sink filters and then in the opposite direction. The flow transient was allowed to decay and the steady-state flow rate was then determined.

To interpret the hydraulic data, inverse modelling was undertaken using the FESTIG 3-D finite element groundwater flow code. Isotropic hydraulic permeability was assumed in all models. A mesh representing one sixteenth of the CVRF specimen was developed using 33,916 tetrahedral elements connecting 9,294 nodes (Figure 4-4).

The model was run for three different test configurations: (A) high pressure (10 MPa) applied to the central filter and low pressure (1 MPa) at the axial and radial filters; (B) low pressure applied to the central filter and high pressure at the axial and radial filters; and (C) high pressure applied to the central filter with low pressure at the radial filters and no flow from the axial filters. The input permeability value was altered until the total flow through the system corresponded to the observed steady-state rate.

Figure 4-4 also shows the steady-state porewater pressure distribution for each of the three test configurations. Hydraulic results are presented in Table 4-2. The average permeability of specimen Mx80-8 from inverse modelling of steady-state flows is found to be 1.4×10^{-21} m^2. Inverse modelling of the rather noisy transient flow data gives an average permeability of 1.7×10^{-21} m^2 and a specific storage in the range 1 to 9×10^{-6} m^{-1}. These values of specific storage are exceptionally small, as one might anticipate for a fully-saturated constant volume system.

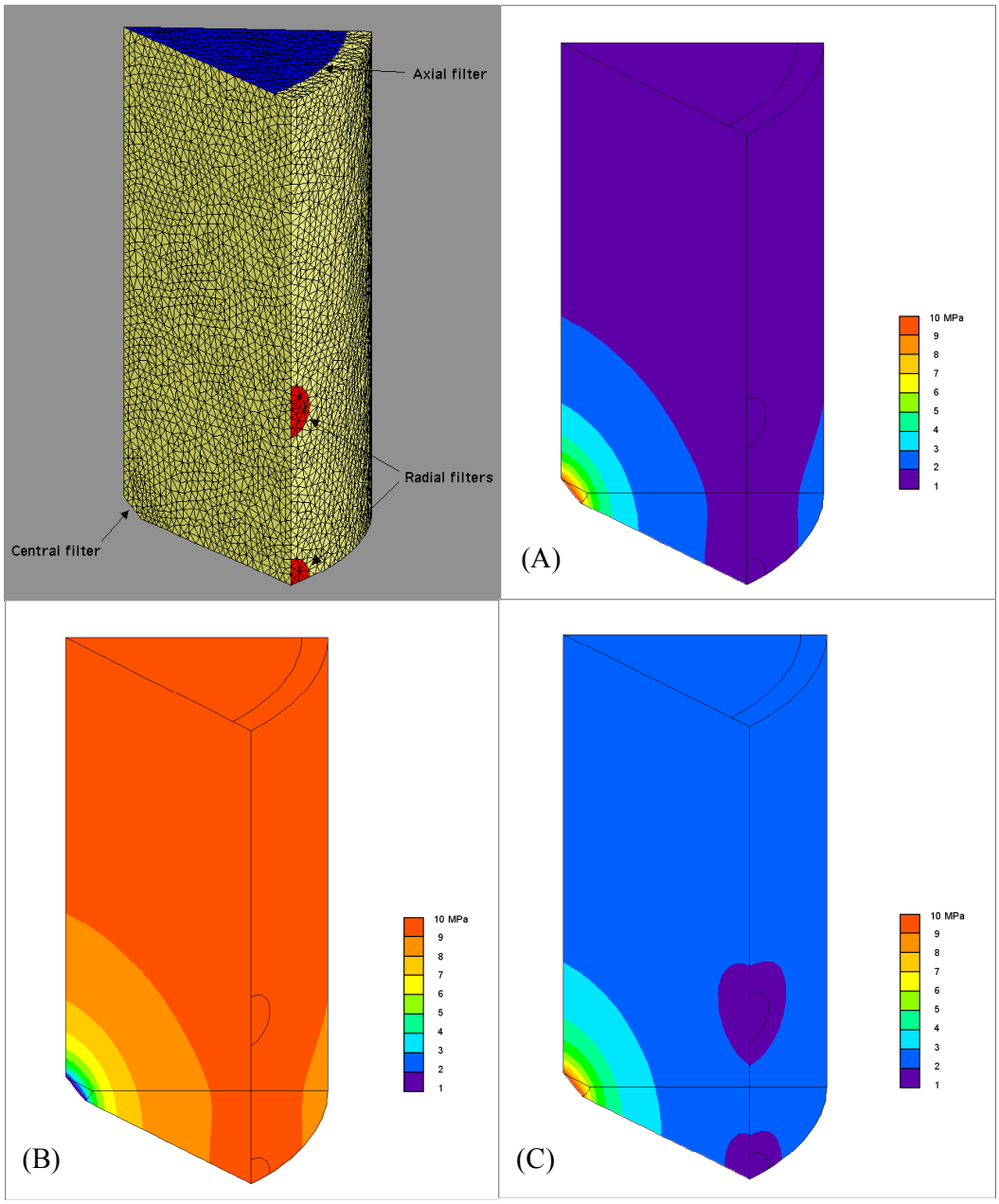

Figure 4-4. *Finite element mesh used to model water flow in specimen Mx80-8 and contours of the steady-state porewater pressure for test configurations (A), (B) and (C).*

Table 4-2. Permeability data for pre-compacted Mx-80 bentonite with a dry density of 1.6 Mg.m^{-3}.

Test number	Test geometry	Test configuration	Applied pressure gradient (MPa)	Steady-state flow rate (μl.hr^{-1})	Hydraulic permeability (m^2 x10^{21})
Mx80-8	CVRF	(A)	9.0	1.34	1.4
		(B)	9.0	2.23	2.3
		(C)	9.0	0.35	0.4
Mx80-9	K_o	–	2.1	2.90	9.5

4.2.2 Permeability under K_0 test conditions

Distilled water was pumped into the clay at a controlled flow rate of 1.0 µl.hr^{-1}. A small hydraulic leak into the injection system from the confining pressure circuit was noted. It seems likely that a small amount of clay-smearing prevented the injection end-cap 'O'-ring from making a perfect seal within the rigid steel sleeve. At near steady-state conditions, the rate of discharge was close to 2.9 µl.hr^{-1}, for a hydraulic gradient of 2.1 MPa (Figure 4-5). This gives a permeability to water of 9.5 x 10^{-21} m^2. The mid-plane porewater pressure transducer registered a steady-state pressure of 1.0 MPa above backpressure, confirming that the pressure gradient along the specimen was linear in accordance with Darcy's Law.

The pressure transient was subsequently analysed using the curve-fitting routine described in /Harrington et al, 2001/. The fitted permeability and specific storage are 8.7 x 10^{-21} m^2 and 3.8 x 10^{-4} m^{-1} respectively. Specific storage is clearly substantially larger than the range established for CVRF conditions, showing that axial swelling in the K_0 geometry has a very profound effect on storage. The significant increase in permeability under K_0 conditions can be partly explained by the decrease in dry density that accompanies axial swelling.

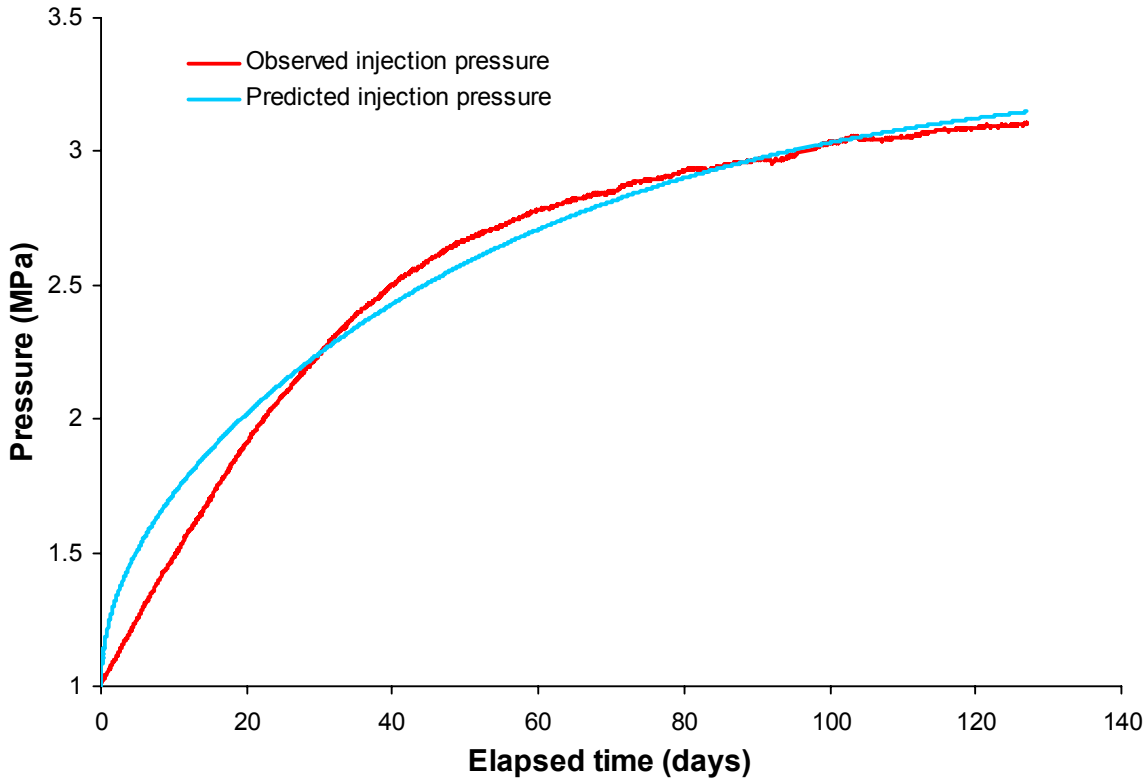

Figure 4-5. *Hydraulic test history for specimen Mx80-9.*

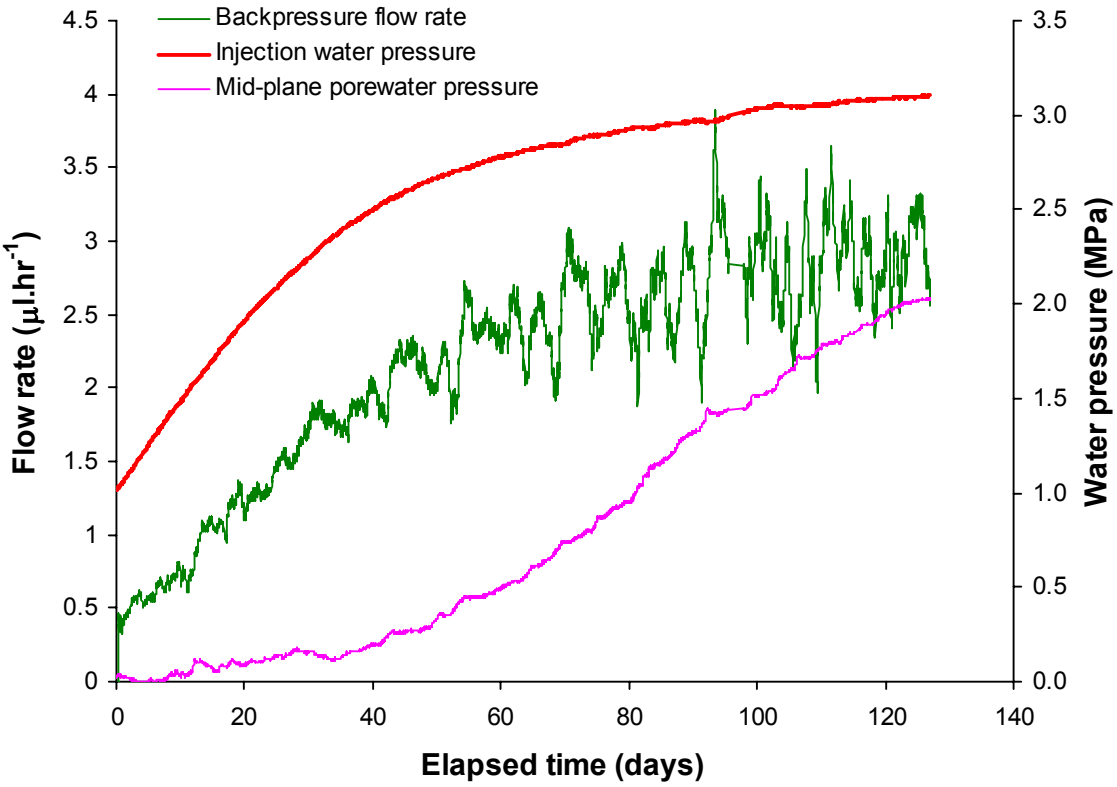

Figure 4-6. *Hydraulic transient from test Mx80-9 showing the best fit line from modelling the non-steady state flow problem.*

4.3 Gas injection results

The results of three gas injection experiments are described in detail. The experimental histories were designed to reveal the main characteristics of the gas migration process, to quantify key parameters and to indicate possible sensitivities to the experimental boundary conditions.

4.3.1 Test Mx80-8

Gas testing began by pumping gas into the upstream system at a rate of 375 µl.hr^{-1}. All filters, other than the central source filter and the radial sink filters, were closed off during gas testing. A very small amount of flow was observed at a gas pressure of 13.8 MPa, accompanied by a slight increase in axial and radial total stress (Figure 4-7). Gas pressure continued to rise until major gas entry occurred at a gas pressure of 18.9 MPa (Figure 4-8). Injection gas pressure momentarily dropped to 18.7 MPa and there was a sharp rise in axial total stress from 1.6 MPa to 18.3 MPa. Gas pressure then continued to rise to a peak value of 19.4 MPa, at which point large quantities of gas began to flow to sink array [1]. It would appear that the first gas pathway did not intersect a sink and a short period of growth was required in order to obtain gas breakthrough.

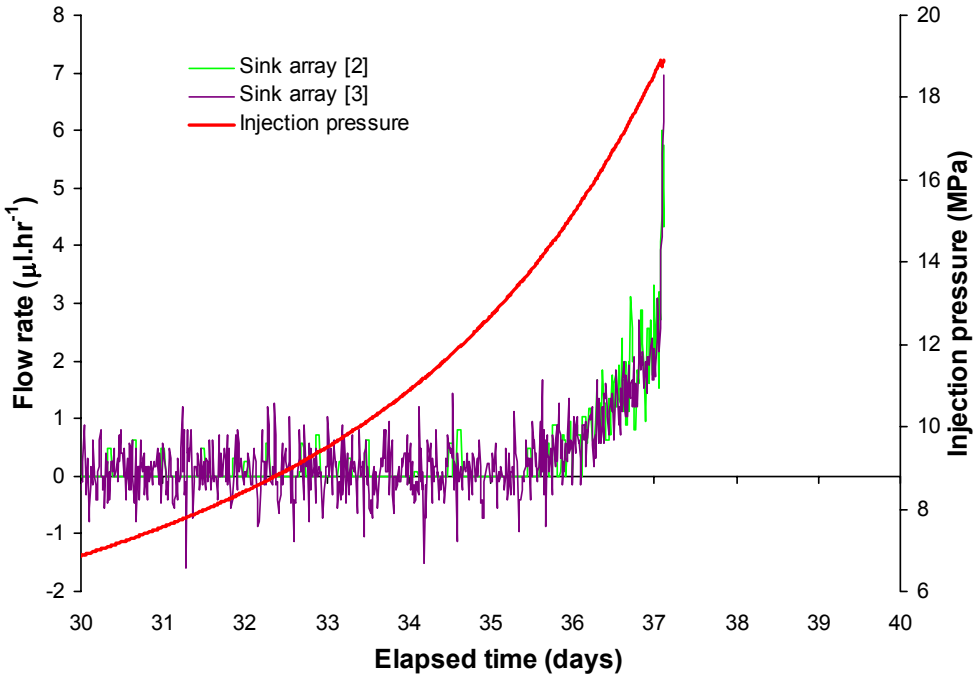

Figure 4-7. *A very small outflow of fluid was observed at a gas pressure of 13.8 MPa during the initial gas injection stage of test Mx80-8. This was accompanied by a slight increase in axial and radial total stress. The leading edge of this response is interpreted as the initial point of gas entry.*

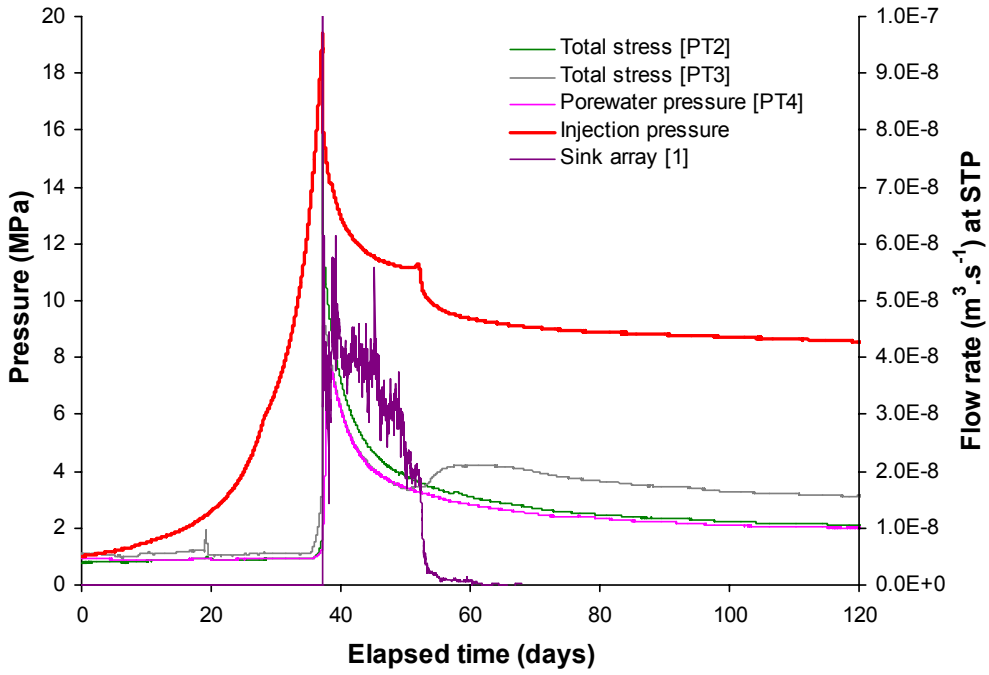

Figure 4-8. *Gas injection pressure versus time for the first breakthrough and shut-in stages of test Mx80-8, showing axial and radial total stress, porewater pressure and flow rate from sink array [1]. Flows to sink arrays [2] and [3] were too small to be distinguished when plotted on this scale. Mass balance considerations show that the flow from sink array [1] is predominantly gas.*

After the peak, steady-state gas flow was observed at a pressure of 11.2 MPa. Approximately 99.9% of the total flow was discharged at sink array [1]. The elevated gas pressure caused a substantial rise in both the porewater pressure and total stress. Figure 4-9 shows the small flux from arrays [2] and [3]. It seems likely that this background flow is exclusively water. The source of this water is examined in section 4.3.4. The injection pump was stopped and gas pressure allowed to decay to delineate the shut-in transient.

Pumping was re-started at the standard rate. As gas pressure increased, both the porewater pressure and total stress began to rise (Figure 4-10). Gas flow was now largely to array [3] which displayed a second major gas breakthrough event at a gas pressure of 9.4 MPa, followed by a succession of small peaks (Figure 4-11). There was no conspicuous post-peak transient and the rate of gas discharge quickly evolved to a steady-state condition at a gas pressure of 11.5 MPa.

The temporal variation in the proportion of gas discharged to each of the sink arrays is worthy of note. The decline in flow to array [3] is followed by an increase in flow to arrays [1] and [2], clearly demonstrating the existence of multiple flow pathways. Extrapolation of the shut-in transient gives an asymptote of around 8.0 MPa. No further gas flow is possible at a gas pressure less than this value.

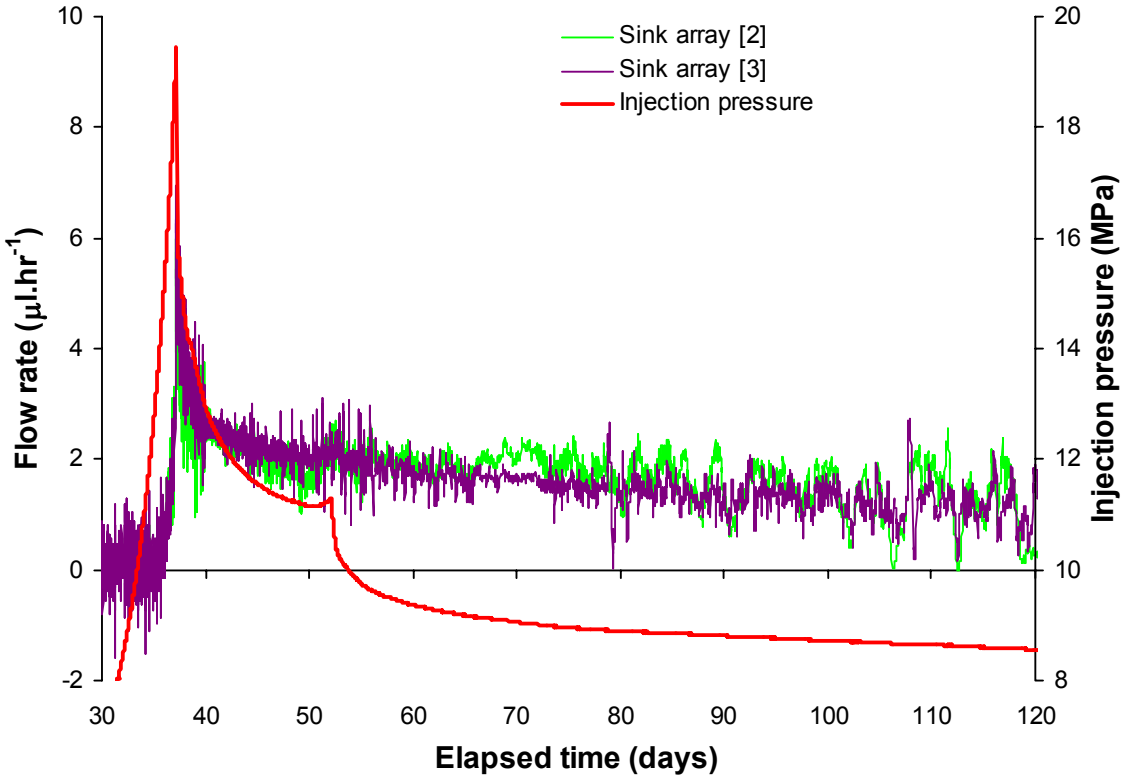

Figure 4-9. *Gas injection pressure versus time for the first breakthrough and shut-in stages of test Mx80-8, showing the small background flow from sink arrays [2] and [3]. It is likely that this flow is exclusively water.*

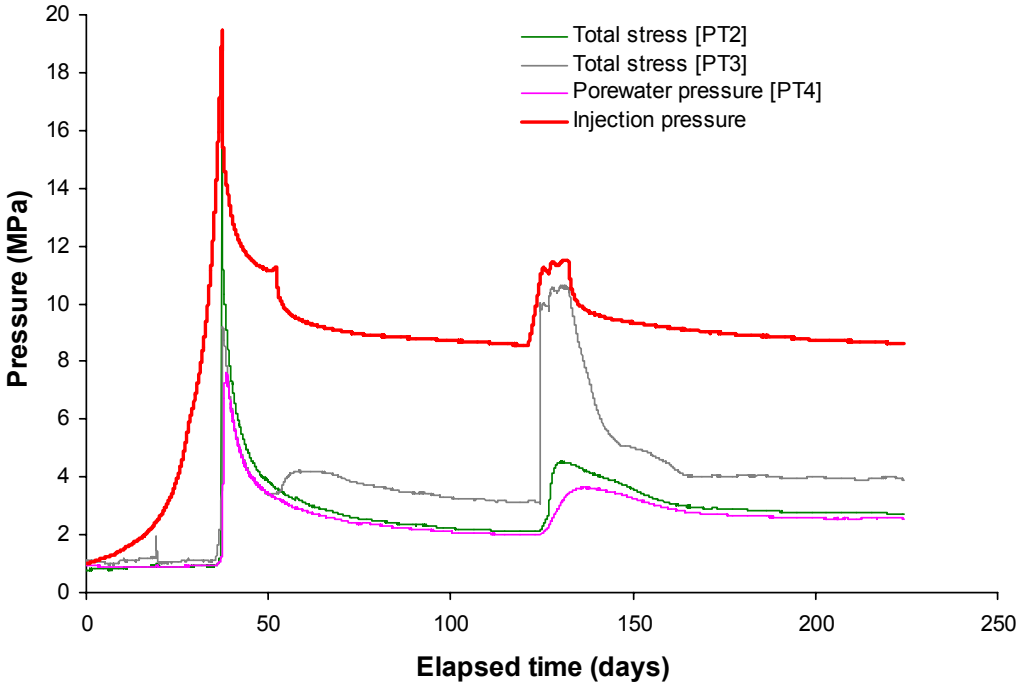

Figure 4-10. *Gas injection pressure versus time for all stages of test Mx80-8, showing total stress and porewater pressure history. Absolute values of stress are thought to be unreliable in this test.*

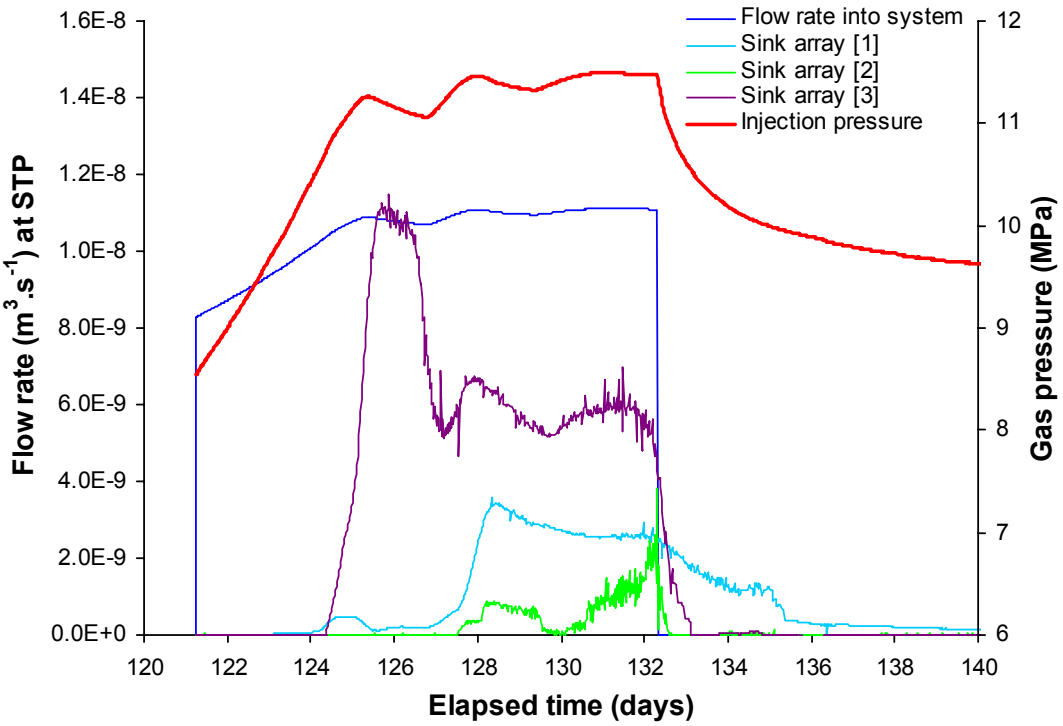

Figure 4-11. *Gas injection pressure versus time for the second breakthrough and shut-in stages of test Mx80-8, showing flow rates into the system and out of the sink filter arrays. Mass balance considerations show that the flows are predominantly gas.*

4.3.2 Test Mx80-9

As in test Mx80-8, gas was pumped into the upstream system at the standardised flow rate of 375 $\mu l.hr^{-1}$. Axial stress and backpressure were held constant at 10.0 MPa and 1.0 MPa respectively. On reaching a gas pressure of 8.8 MPa, the pump was set to supply constant pressure. Outgoing flux was monitored for the next 88 days. Flow rate increased to a peak and then gradually declined (Figure 4-12). This is interpreted as a 'slug' of fluid moving through the specimen. The mid-plane porewater pressure sensor responds to the passage of this slug of fluid, rising to a peak value of 4.1 MPa and then dropping to 2.5 MPa. There was a time-lag of about three days between the flow peak and the pressure peak. By the end of the test stage, the flow rate had declined to 0.1 $\mu l.hr^{-1}$. The significance of the 'slug' of fluid is discussed in detail in section 4.3.4.

Gas pumping was re-started at 375 $\mu l.hr^{-1}$. After only 1 day, major gas breakthrough occurred at a peak pressure fractionally below 10.0 MPa (Figure 4-13). Pressure dropped away very rapidly in the post-peak region. There is evidence of an 'undershoot' in the pressure transient. /Harrington and Horseman, 1999/ considered this type of behaviour to be indicative of the instability of conductive gas pathways. Gas pressure then rose to 8.8 MPa.

At this point in the history, the pumping rate was reduced to 180 $\mu l.hr^{-1}$. The resulting pressure transient also exhibited an 'undershoot'. Gas pressure rose to 8.8 MPa. The injection pump was stopped and the upstream pressure allowed to decay along a shut-in transient. The resulting curve is sufficiently well defined to allow a rough estimate to be made of 8.2 MPa for the zero flow rate asymptote.

After delineating the shut-in transient, the injection pump was restarted at the standardised pumping rate of 375 $\mu l.hr^{-1}$. Flow out of the specimen commenced at a gas pressure around 8.5 MPa. Gas pressure increased to a peak of 9.3 MPa (Figure 4-14). The post-peak transient decayed to a near steady-state pressure of 9.2 MPa. The outgoing flow rate evolved to a plateau with no conspicuous peak. The injection pump was stopped again to provide a second shut-in transient. The break in the slope of the shut-in transient is suggestive of spontaneous closure of flow pathways. The projected zero flow rate asymptote is around 8.0 MPa (Figure 4-15).

During the major gas flow events, the output of the mid-plane porewater pressure sensor remained fairly constant at 2.5 MPa (i.e. 1.5 MPa above the backpressure) and the sensor did not show any obvious sensitivity to changes in upstream gas pressure or pumping rate. It seems likely that gas penetrated the filter and tubing leading to a substantially reduced sensitivity of the measuring system to porewater pressure changes.

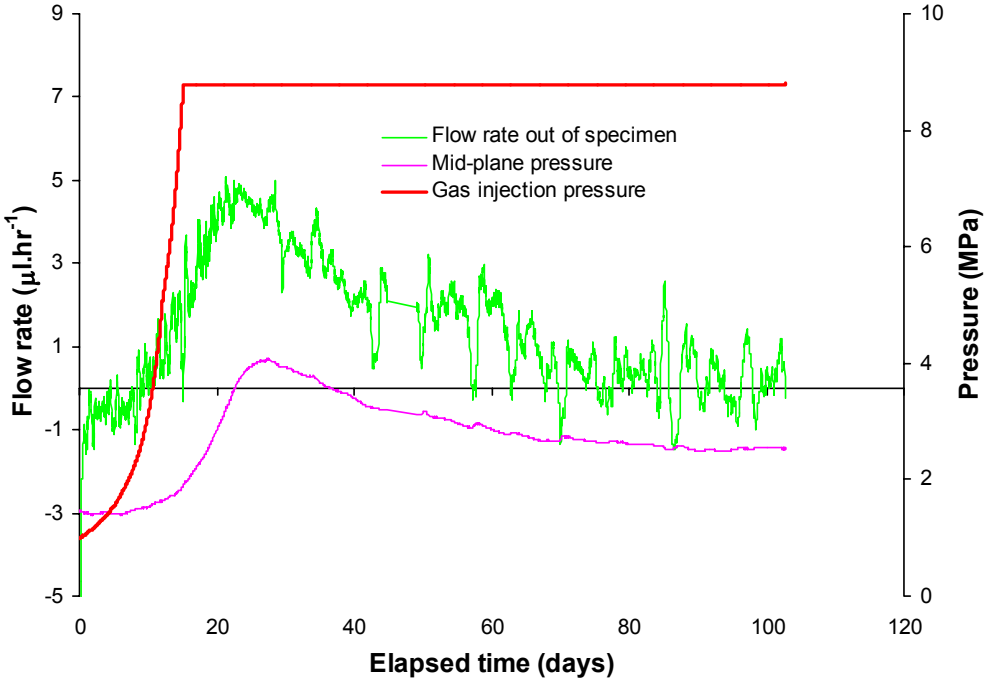

Figure 4-12. *First 100 days of test Mx80-9 showing the pumping stage and 8.8 MPa constant gas pressure stage. The monitored outflow and the correlated response of the mid-plane porewater pressure sensor are interpreted in terms of a slug of water displaced from the upstream filter and connecting tubing..*

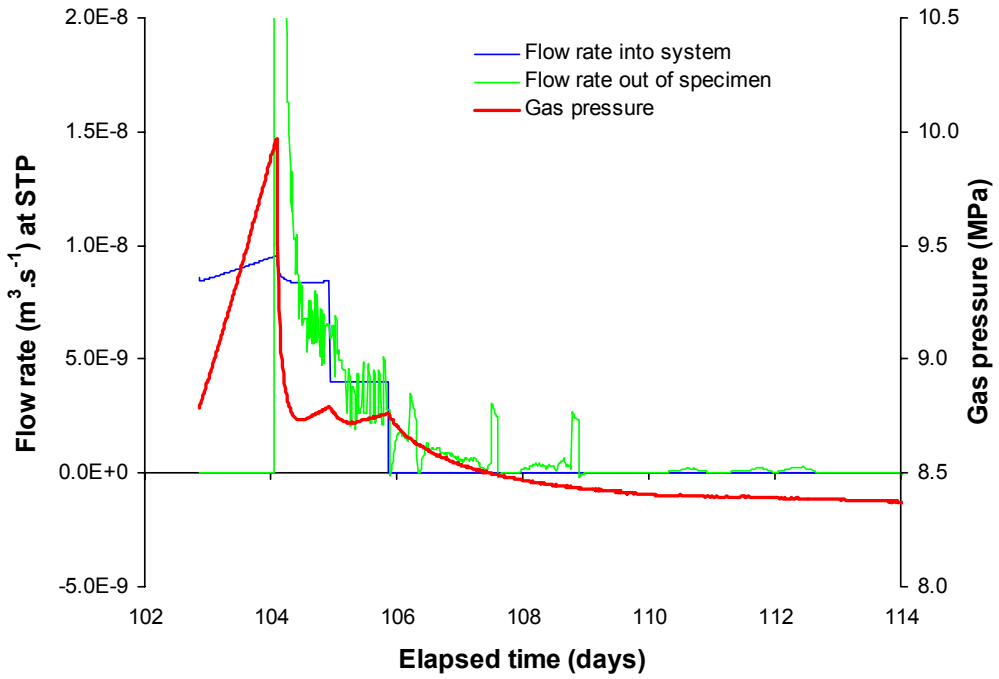

Figure 4-13. *Gas injection pressure versus time for the controlled flow rate and shut-in stages of test Mx80-9, showing flow rate into the system and out of the specimen. The main breakthrough event is at a gas pressure fractionally less than the axial stress applied to the specimen. Mass balance considerations confirm that the flows are predominantly gas. Gas cannot be mobile in the bentonite at a pressure less than the asymptote of the shut-in transient.*

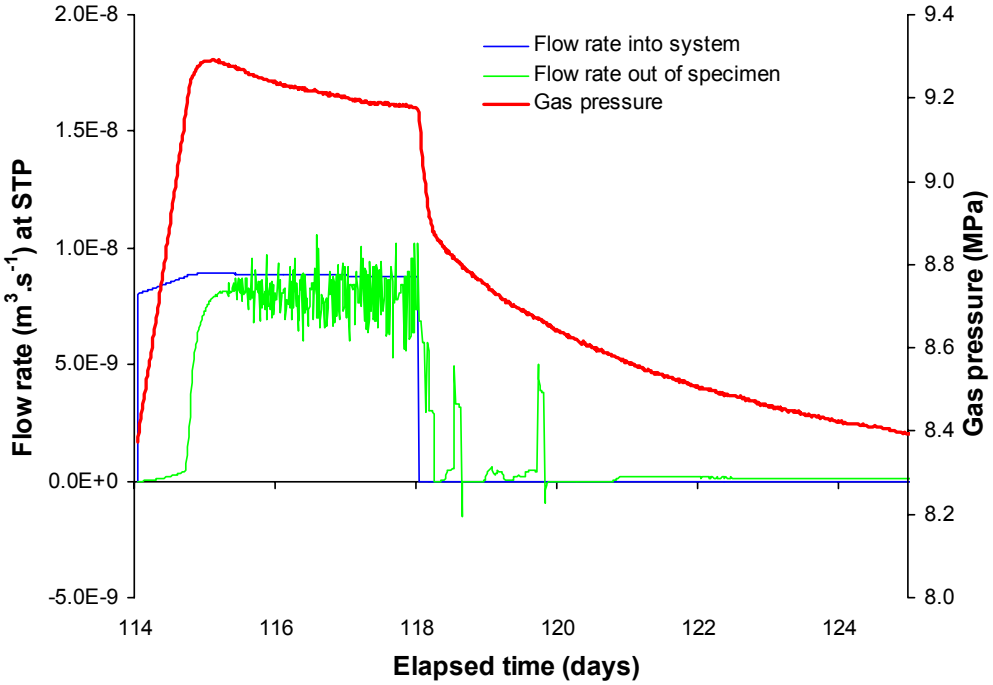

Figure 4-14. *Gas injection pressure versus time for second breakthrough and shut-in stages of test Mx80-9, showing flow rate into the system and out of the specimen. Mass balance considerations show that the flow is predominantly gas. The break in the slope of the shut-in transient is suggestive of spontaneous closure of flow pathways.*

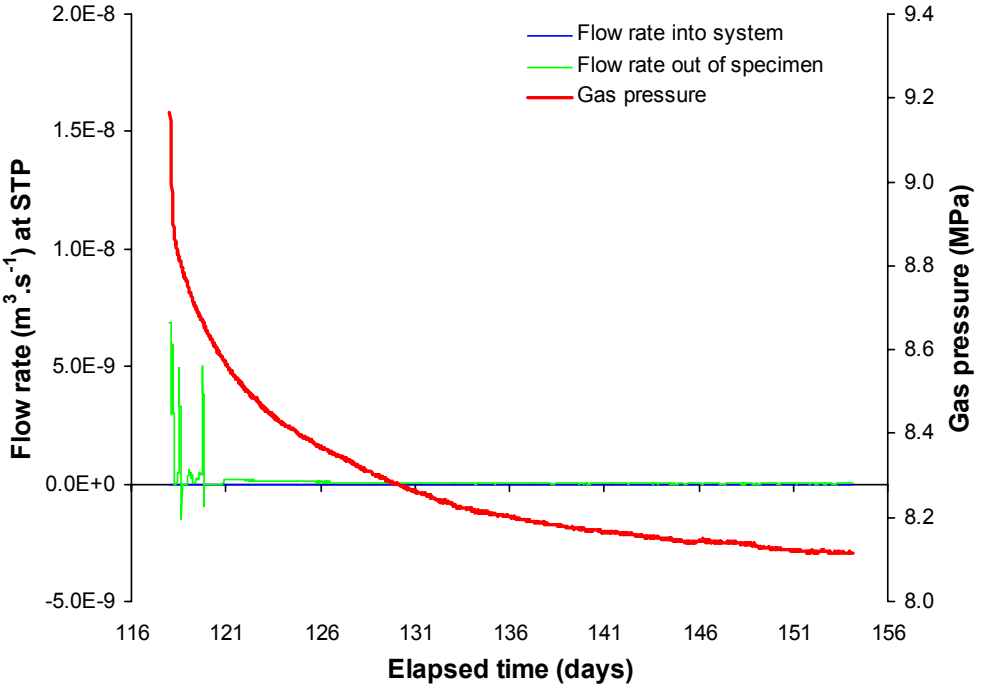

Figure 4-15. *Complete history of the second shut-in stage of test Mx80-9, showing flow rate into the system and out of the specimen. The asymptote of the curve is taken to be around 8.0 MPa.*

4.3.3 Test Mx80-10

Gas was pumped into the injection system at the standard rate of 375 $\mu l.hr^{-1}$. When gas pressure reached 6.0 MPa (after 27 days), it was held constant for a further 33 days. A small outflow was observed, equally distributed between the sink arrays. The significance of this outflow is examined in section 4.3.4. Pumping was restarted at the standard rate. At a gas pressure around 8.6 MPa, the flow rate to each of the radial sinks began to increase. This was accompanied by a slight rise in porewater pressure and a small increase in total stress at most of the sensors. Flow continued to be evenly distributed between the sinks. When gas pressure reached 11.0 MPa (after 70 days of testing), the injection pump was again stopped and the upstream gas pressure held constant. Shortly after stopping the pump, the rate of discharge to all sink arrays increased. Major gas breakthrough was marked by an increase in total stress at all sensors (Figure 4-16). The outflow of gas was non-uniformly distributed between the three sink arrays, with flow maximum in array [3] and minimum in array [1]. This correlates with the response of the stress sensors, which show the highest changes near the injection end-closure [PT2] and the lowest near the backpressure end-closure [PT1].

The post-peak response of the axial total stress sensor [PT2] in Figure 4-16 shows a spontaneous negative transient characteristic of gas breakthrough events seen in previous tests /Harrington and Horseman, 1999/. The rise in total stress and the subsequent increase in flux are indicative of gas penetration of the buffer fabric and the rapid growth of conductive gas pathways. The strong coupling between total stress and gas pressure signifies an overall tendency for the clay to dilate as the gas pathways develop. The non-uniform distribution of the discharge across the sinks is proof of pathway flow through channels of varying conductivity. Gas penetration of the specimen occurred at a gas pressure in the range 8.6 to 8.8 MPa.

After 124 days of testing, the injection pump was reset to deliver the standard pumping rate of 375 $\mu l.hr^{-1}$. The discharge rate to sink array [3] increased immediately, while discharge to arrays [1] and [2] exhibited a time lag of around two to three days before they too began to increase (Figure 4-17). The stress sensors showed step-like responses which correlate with discrete propagation events (Figure 4-18). Since there was no corresponding increase in the discharge of gas to the sinks, it can be inferred that none of the induced pathways actually intersected sink filters.

When gas pressure reached 16.0 MPa, the pump was switched back to constant pressure mode. After 27 hours, gas flow to sink arrays [1] and [3] spontaneously increased and both downstream pumps completely filled with gas in a period of only 30 minutes. The injection pump ran out of gas and some water was pumped into the injection filter.

Another pre-charge of gas was placed in the injection pump, the system gas flushed, and gas pumping re-instated at the standard rate of 375 $\mu l.hr^{-1}$. As gas pressure began to rise, there were no obvious sign of flow out of the specimen from sink arrays [1] and [3] which had previously been so gas conductive (Figure 4-19). This demonstrates that it is possible to ‘reseal’ the clay and regain the peak pressure response by the simple expedient of re-injecting water. At around 136 days, the total stress sensor [PT5] began to slowly increase with time. Similar, but less pronounced, behaviour was seen in stress sensors [PT3] and [PT6] and in porewater pressure sensor [PT4].

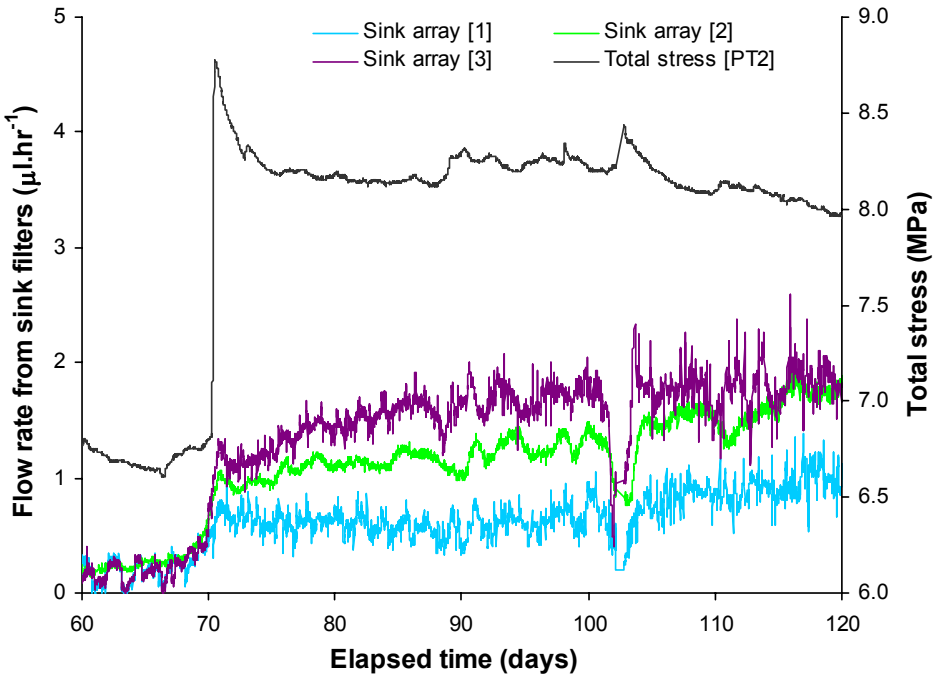

Figure 4-16. *Gas breakthrough in test Mx80-10 at a fixed gas pressure of 11.0 MPa. The breakthrough event is marked by a large change in the total stress acting on the clay. Outflow is non-uniformly distributed between the sink filter arrays.*

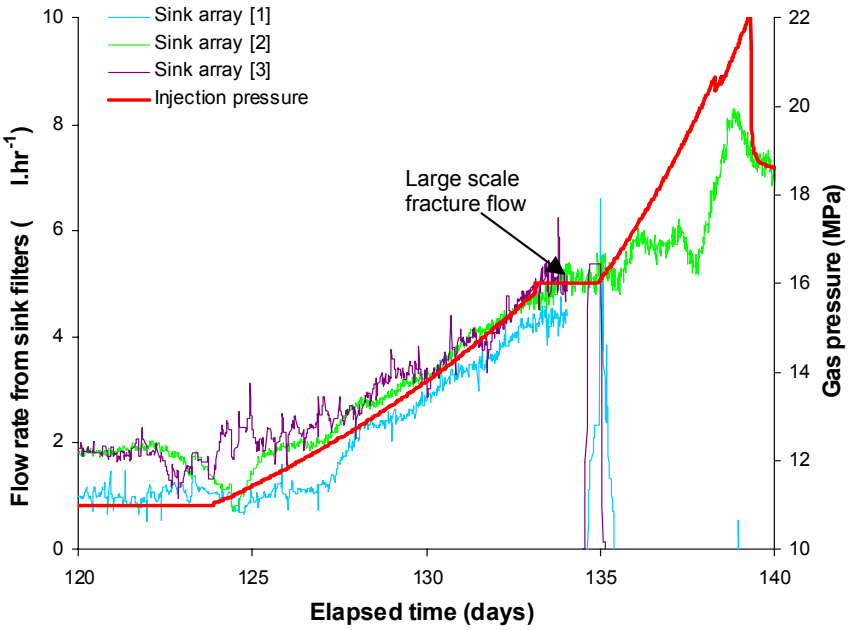

Figure 4-17. *Next phase of test history Mx80-10, showing the injection gas pressure plotted against elapsed time and the flow rate from each sink array. At around 134 days, large-scale gas flow was detected from arrays [1] and [3]. The height of the gas pressure peak is probably pumping-rate dependent.*

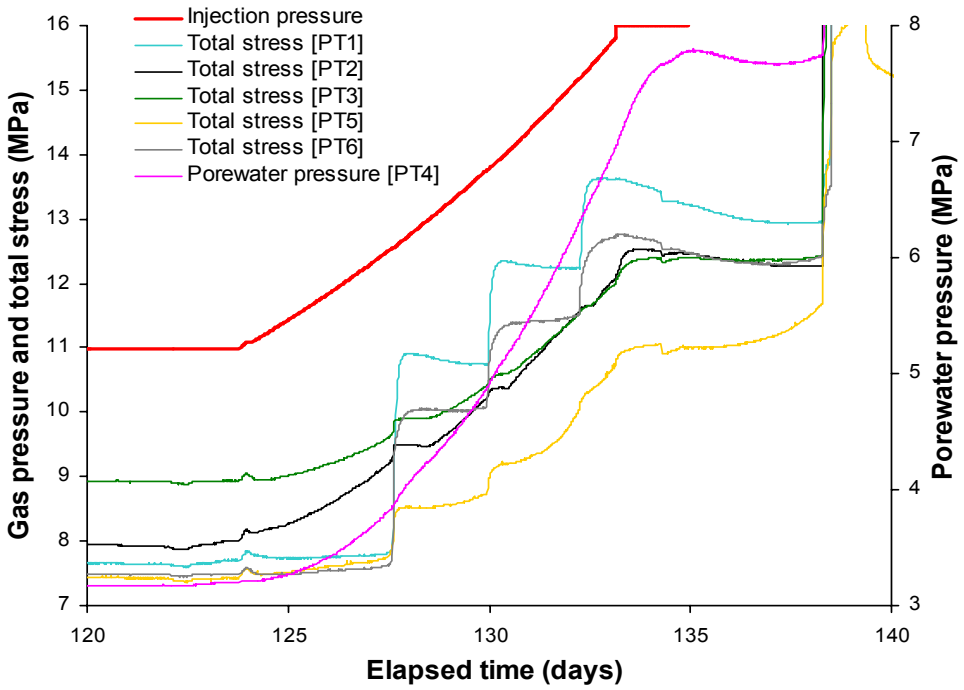

Figure 4-18. *Response of the total stress and porewater pressure sensors over the same test period as depicted in Figure 4-17. Note the substantial increase in porewater pressure and the step-like changes in stress. These steps in stress are indicative of gas pathways which propagate through the clay, but fail to intersect a sink filter.*

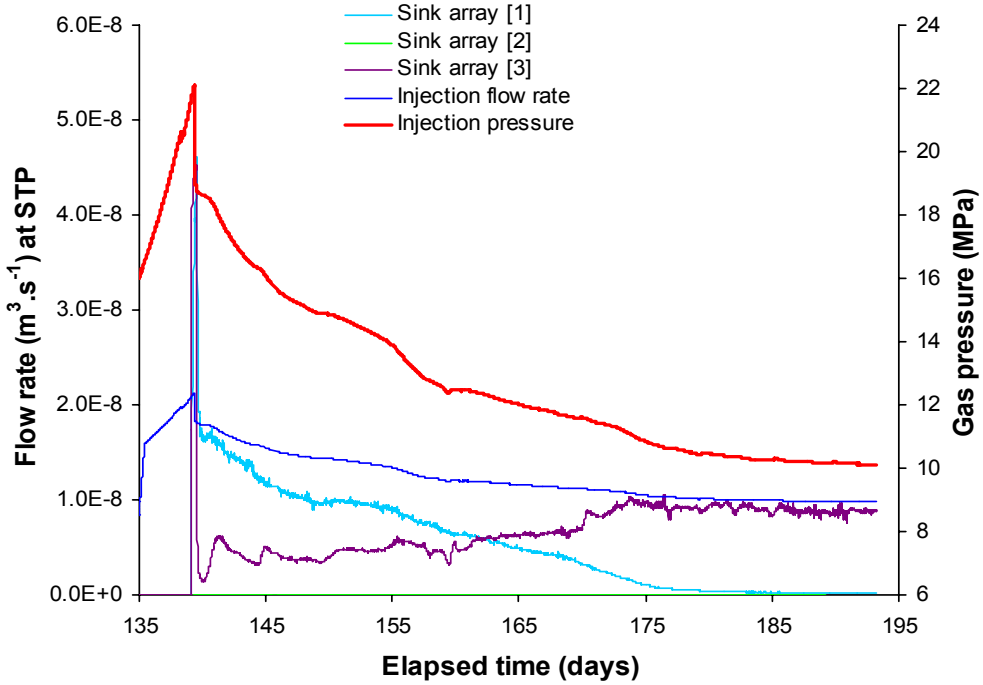

Figure 4-19. *Post-peak transient of the controlled flow-rate stage of test Mx80-10 showing the STP flow rates into the system and out of the sink array. Mass balance considerations confirm that the flow is predominantly gas. The pressure transient approaches an asymptote at the (near) steady-state condition at which flow rate into and out of the specimen are approximately equal. The sharp drop in pressure immediately after the peak is suggestive of a breakdown of tensile strength.*

The was a small, but abrupt, drop in the injection gas pressure at 138 days, accompanied by a dramatic increase in the outputs of all stress and porewater pressure sensors (Figure 4-20). This increase is greatest at [PT2] which is axial stress at the injection end-closure. There is no doubt that the abrupt momentary drop in gas pressure is a consequence of fracture propagation. Since this event was not accompanied by large-scale gas flow, it is clear that the fracture failed to intersect any of the sink filter arrays.

There was a second small drop in injection pressure a few hours after the first, marking the propagation of a second gas fracture from the source filter. Gas pressure then continued to rise, reaching a peak of 22.1 MPa. At this point, major gas breakthrough occurred to sink arrays [1] and [3]. Peak gas pressure was around 2.7 MPa above the maximum stress registered by sensor [PT2]. After breakthrough, gas pressure and total stress showed another abrupt drop, with porewater pressure gradually falling away. During the post-breakthrough period, gas pressure is actually equal to the axial total stress as registered by sensors [PT1] and [PT2]. This shows that the first fully-conductive gas fractures had more or less radial orientations. Conventional interpretation of the post-peak response using hydrofracture theory would suggest that the tensile strength of the bentonite is around 2.7 MPa.

From the gas entry event at a total elapsed time of around 70 days to the region of the peak, the injection gas pressure is around 8.0 ~ 9.0 MPa above the porewater pressure, with a small departure from this situation at around 135 days. As the gas gradually penetrates the clay, it would appear to drive up the water pressure.

After the abrupt post-peak drop, gas pressure slowly declined towards a steady-state value of around 10.1 MPa. The pressure transient shows a number of discrete breaks in slope which are indicative of changes in pathway conductivity. There is evidence that some degree of pathway self-sealing was occurring. The gas pressure throughout the transient is close to the average total stress acting on the specimen (Figure 4-21). This is in contrast to the pre-peak behaviour where gas pressure was consistently well above the average total stress.

The injection pump was switched off and the gas pressure allowed to decay. Breaks in the slope of the shut-in curve coincide with reductions in gas discharge rate, providing confirmation of pathway self-sealing. Throughout much of the shut-in transient, the gas pressure exceeds the porewater pressure by around 5.8 MPa. The output of the porewater pressure sensor drifted gradually upward at the end of the stage due to gas penetration of the porous filter. The zero flow rate asymptote is estimated to be around 7.0 MPa.

The test stage was stopped after 507 days and gas was removed from injection and backpressure systems and replaced with de-aired distilled water. A hydraulic test was performed using the same method as for specimen Mx80-8 (see section 4.2.1). The water pressure in the injection system was set at 10.0 MPa while the backpressure was maintained constant at 1.0 MPa. Early breaks in slope of the volumetric flow rate response after 1 and 9 days indicate a reduction in hydraulic permeability as water entered the clay, occupying previously gas-filled voids (Figure 4-22). The initial rise in total stress is due to the increase in water pressure in the region of the central injection filter. Since only a small proportion of the rise in water pressure was observed at the stress sensors, the gas must have been resident within the clay fabric. By the end of the test stage, an average total volumetric outflow of 1.4 $\mu l.hr^{-1}$ was observed from both the sink and end-closure filters. This is the same as the average steady-state outflow

observed during the hydraulic tests on specimen Mx80-8 prior to gas testing, indicating that the development of gas pathways has no long-term detrimental effect on permeability to water and the overall sealing properties of the buffer clay.

To further examine the self-sealing capacity of the bentonite, another pre-charge of gas was placed in the injection pump and the system gas flushed. Gas pumping was re-instated at the standard rate of 375 µl.hr^{-1}. As gas pressure began to rise, there were no obvious signs of flow out of the specimen from sink arrays [1] and [3] which had previously been gas conductive (Figure 4-23).

When injection pressure reached 9.4 MPa, a small outflow was detected at each of the sink arrays, along with a small increase in total stress (Figure 4-24). Another fracture propagation event was marked by a sharp rise in the total stress measured at sensors [PT2] and [PT3]. This event coincided with a small change in the slope of the gas pressurisation curve. The peak pressure was 12.8 MPa which is substantially lower than the previous value of 22.1 MPa. The abrupt drop in pressure after the peak is suggestive of another breakdown in tensile strength. It seems likely that the clay regained some of its strength in tension during the preceding rehydration phase. This can also be interpreted in terms of a fracture 'self-sealing' mechanism.

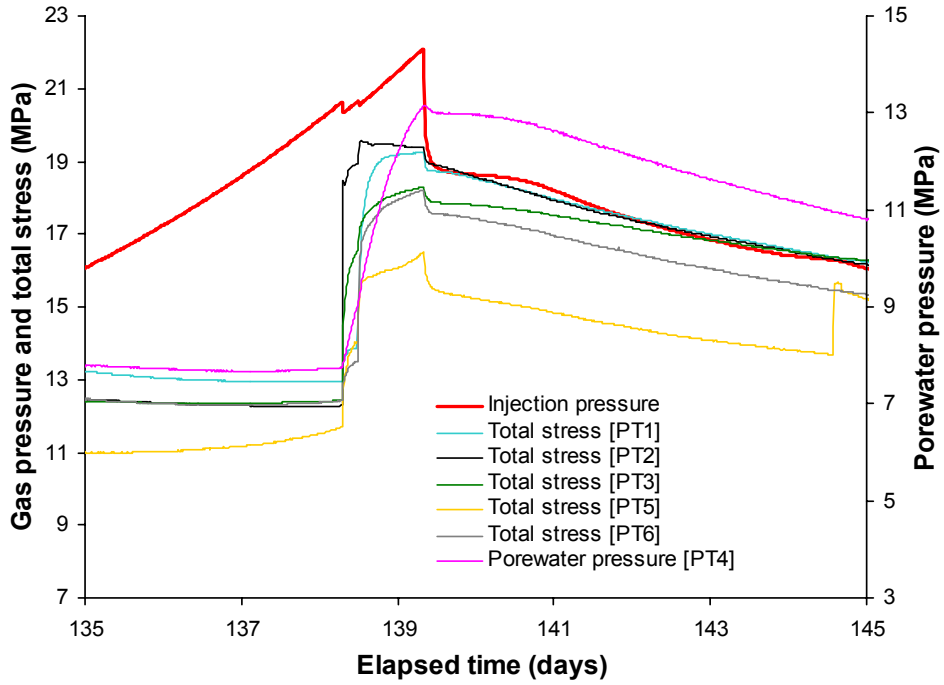

Figure 4-20. *Detail of the region of the peak in the controlled flow-rate stage of Mx80-10 showing the variations in total stress and porewater pressure responses during initial major gas entry and subsequent breakthrough events. The abrupt drops in gas pressure before the peak are indicative of pathways which propagate but fail to connect with the sink filters.*

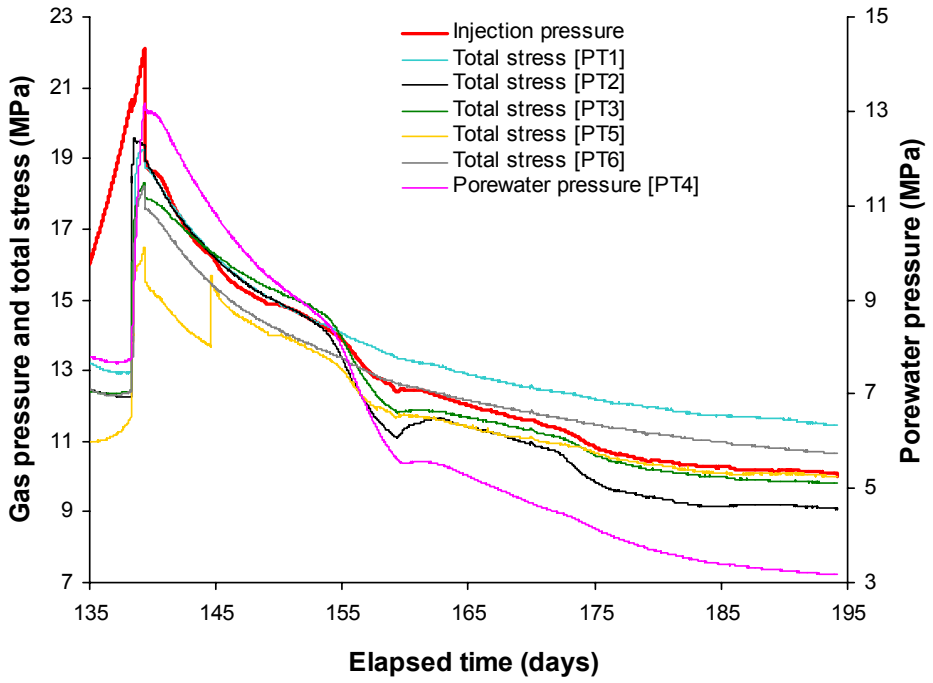

Figure 4-21. *Post-peak transient of the controlled flow-rate stage of test Mx80-10 showing variations in total stress and porewater pressure. In the post-peak region, the injection gas pressures has a value close to the average total stress on the specimen.*

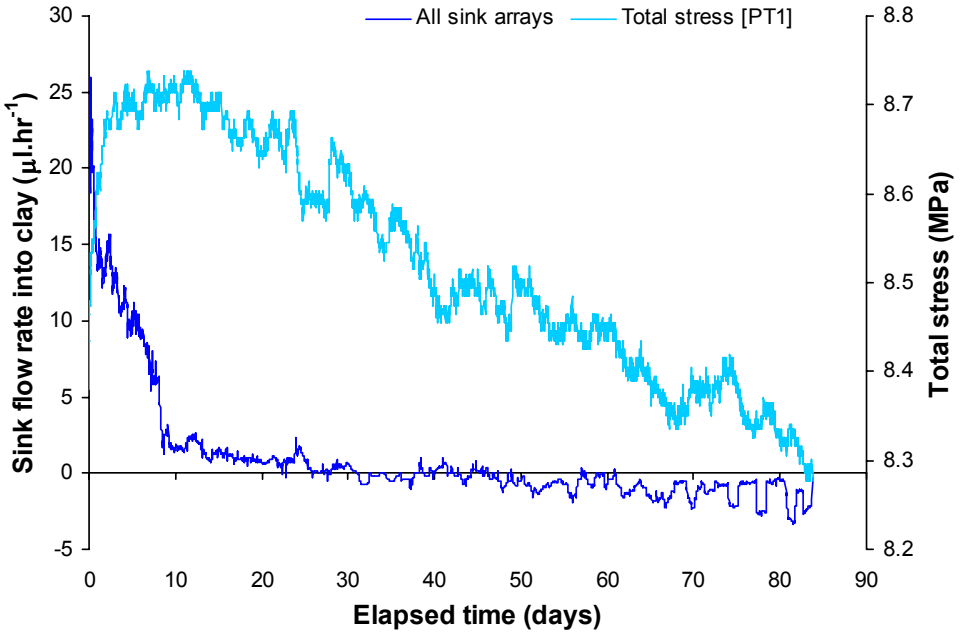

Figure 4-22. *Rehydration of experimental history Mx80-10 after the first gas injection test, showing cumulative flow rate into/out of the specimen and the total stress response of [PT1].*

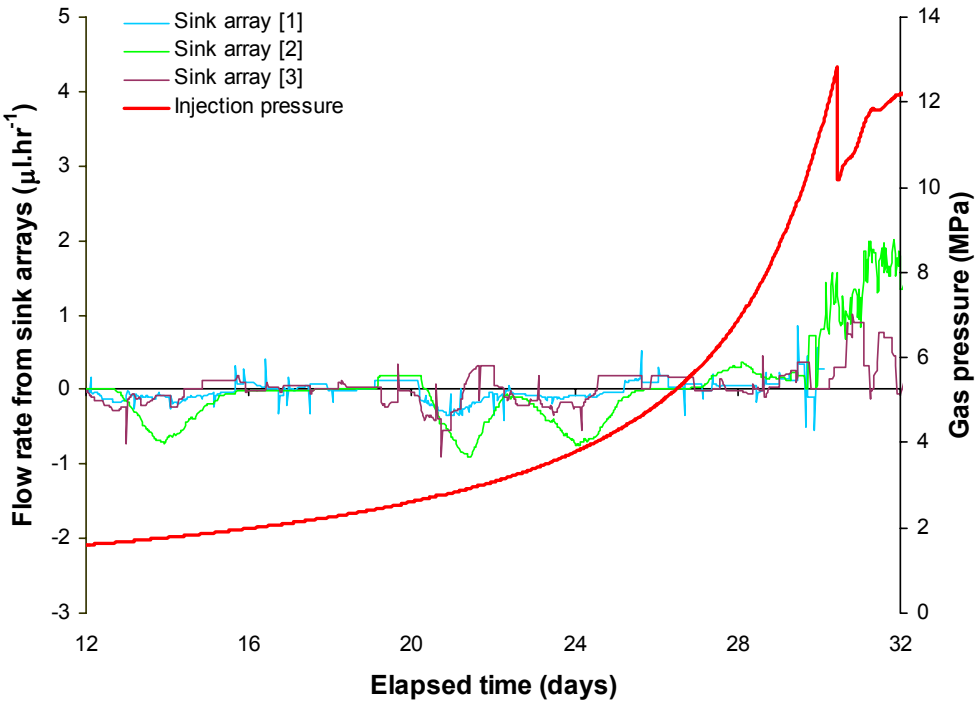

Figure 4-23. *Gas injection pressure versus time for the final gas injection phase of test Mx80-10, showing flow rates from the sink filter arrays. The peak pressure is 12.8 MPa and is substantially lower than the previous value of 22.1 MPa.*

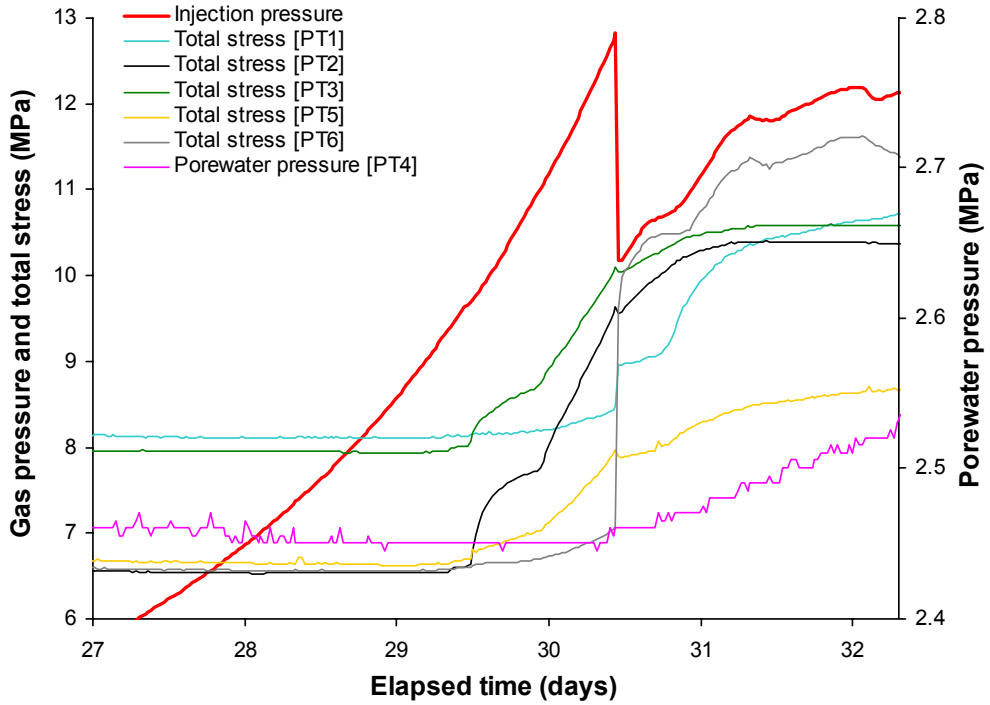

Figure 4-24. *Detail of the final gas injection phase of test Mx80-10, showing variations in total stress and porewater pressure during breakthrough. The abrupt drop in pressure after the peak is suggestive of a breakdown of tensile strength. It seems likely that the clay regained some of its strength in tension during the preceding rehydration phase.*

4.3.4 Evidence for porewater displacement

It has been suggested by others that the rate of gas pressurisation in laboratory experiments on bentonite is usually so large that gas fracturing becomes the dominant mechanism of gas transport, and advective transport of gas in original pores therefore remains undetected. By implication, if the experiments were to be performed over a substantially longer time period than is currently the case, then gas at only modest pressure would progressively displace water from the original pores of the bentonite in accordance with the predictions of two-phase flow theory.

Special consideration has been given to this issue. Table 4-3 shows the mass of the test specimens before and after gas testing and the total amount of gas passed through the specimens. It can be seen that, in all cases, the water content of the specimens actually increased over the course of gas testing. This can be attributed to resaturation of the starting material during the hydration and hydraulic testing stages of each test (Table 4-4). The specimens were exposed to gas pressures greater than 8 MPa for periods of time ranging between 5 and 13 months. The masses of specimens Mx80-8 and Mx80-9 were measured immediately after completion of gas testing. What is absolutely clear from these results is that it is possible to pass up to 60 litres (STP) of helium through specimens of buffer clay without any measurable desaturation occurring. This strongly reinforces the observations made by /Pusch and Forsberg, 1983/ on the absence of desaturation during gas flow in Mx80 bentonite.

Table 4-3. Change in mass of the specimens over the full testing history.

Test specimen	Specimen mass (g)		Increase in mass (g)	Increase as % of pre-test mass	Total gas flow at STP (litres)
	Pre-test	Post-test			
Mx80-8	674.34	678.07	3.73	0.55%	55.5
Mx80-9	206.43	207.97	1.54	0.75%	4.5
Mx80-10	676.86	680.37	3.51	0.52%	60.4

Table 4-4. Changes in saturation over the full testing history.

Test specimen	Initial saturation (%)	Initial volume of gas voids (cm^3)	Net inflow of water (cm^3)	Final saturation (%)	Time period at over 8 MPa (days)	Comments
Mx80-8	97.6	3.49	3.73	100.2	195	Constrained
Mx80-9	98.3	0.89	1.54	101.4	139	Free to swell axially
Mx80-10	98.9	1.59	3.51	101.3	390	Constrained

In test Mx80-8, the first signs of gas entry were observed at a gas pressure of 13.8 MPa (see section 4.3.1). By careful processing of the discharge flow rate data before the entry event using moving-average smoothing, it is possible to discern a very small emergent flux ($\leq$0.1 $\mu l.hr^{-1}$) from each of the sink arrays. This barely resolvable flux tends to decline with time and is not correlated with injection gas pressure, monitored porewater pressure or total stress. The total amount of fluid flow is estimated to be 0.13 ml over 20 days.

A qualitatively similar response was observed in test Mx80-9 (see Figure 4-12). The flow rate and the mid-plane porewater pressure show pronounced peaks. It is clear that the flow is a response to the gradient in porewater pressure. Using the measured value of hydraulic permeability, the flow rate can be predicted from the pressure gradient. Collectively, these observations suggest that the background flow in this test is exclusively water.

The first constant gas pressure (6.0 MPa) stage of Mx80-10 was designed to provide additional information on this early stage behaviour. The response is similar to that of the Mx80-8, with an outgoing flux ($\leq$0.2 $\mu l.hr^{-1}$) detectable at each of the sink arrays. This flux declined slowly with time. Porewater pressure at the [PT4] sensor increased by 0.3 MPa over the same period and then gradually dropped away as the flux declined. The total stress sensors showed no response to the change in porewater pressure. The total amount of the outgoing flow is estimated to be 0.38 ml over 37 days.

There is no doubt that the outflow seen at the downstream filters in the early stages of these tests was water. The important observations are the lack of correlation with the injection gas pressure and the overall decline in the flow rate with time. If this flux were to represent porewater displaced from the clay by gas movement into original pores, one would anticipate that the flow rate would rise with time and with increasing gas pressure. This was not the case. It is suggested that the very small amounts of water that passed to the downstream filters at injection gas pressures less than the stated entry pressures were artefacts of the experimental method. At the commencement of gas testing, efforts to flush the injection system of water were not totally effective and a little water remained trapped in the pores of the upstream filter and in the connecting tube. This slug of water was driven through the clay during the early stages of the test. Once the source was depleted, the emergent flow rate at the sink arrays declined.

Once gas has penetrated the clay it is possible to displace water from other filters incorporated in the experimental design. Table 4-5 gives the total amount of pore space provided by these filters. Inspection of this table reveals that the large end-closure filters used to hydrate the specimen in CVRF testing can act as substantial reservoirs of water.

Recalling some of the details of test Mx80-8, it was observed that during the first gas breakthrough event the gas flowed to sink filter array [1]. However, inspection of Figure 4-9 reveals a small background flow to sink filters [2] and [3]. This flow is believed to comprise exclusively water. The total flow from the breakthrough to the end of the shut-in is around 6.8 ml. If this flow were indicative of the displacement of porewater by gas, we would anticipate the mass of the specimen to decrease during gas testing by at least 6.8 g. It is clear from Table 4-3 that there was no decrease in mass.

Table 4-5. Pore space of filters based on a sinter porosity of 55%.

Test number	Filter	Volume of filter (ml)	Volume of pore space (ml)	Total volume of pore space (ml)
Mx80-8	Injection end-closure	12.38	6.20	13.76
	Backpressure end-closure	13.74	7.56	
	Source filter	0.10	0.06	0.06
	Sink filter (x12)	0.75	0.41	4.96
Mx80-9	Injection end-cap	12.21	6.71	13.42
	Backpressure end-cap	12.21	6.71	
Mx80-10	Injection end-closure	12.38	6.20	13.08
	Backpressure end-closure	13.06	6.88	
	Source filter	0.10	0.06	0.06
	Sink filter (x12)	0.75	0.41	4.96

Since there was no indication of an inflow of water from any of the pumps that might compensate for the measured outflow, the flow to the sink arrays in Figure 4-9 must be traceable to an alternative source. In the CVRF tests, the end-closure filters provide this alternative source of water. As gas pathways propagate through the clay, it is inevitable that some will intersect the end-closure filters. Since these are water saturated and isolated from the pumps, gas flowing into the pore space of one of these filters will raise the water pressure. The water will be displaced through the clay to the sink array filters. Flow must cease when the filter becomes gas saturated. This gas will remain trapped in the filter pore space during the subsequent test stages.

Table 4-4 provides the most important observations on the issue of bentonite desaturation during gas flow. After intense scrutiny of the experimental data, we are unable to present any convincing evidence of porewater displacement, desaturation or conventional two-phase flow in buffer bentonite. We would note, however, that a strong case can be made for some small degree of bentonite de-watering by internal consolidation of the clay mass when gas has fully penetrated the bentonite and the gas pressure within the flow pathways exceeds the sum of the swelling pressure and the externally-applied water pressure.

5 Process understanding

Gas entry, breakthrough, peak and steady-state gas pressures are systematically higher under constant volume boundary conditions than they are under the radially-constrained (i.e. K_0) conditions. These quantities are also conspicuously larger than those measured under the constant total stress boundary conditions of the tests reported in /Horseman et al, 1997, 1999/. This strongly suggests that the process of gas entry is accompanied by dilation of the bentonite fabric (i.e. a tendency for the volume of the specimen to increase). The increases in porewater pressure and total stress under constant volume conditions are a direct consequence of the constrained dilatant response.

After gas entry but before the pressure peak, the gas pressure under constant volume conditions can rise to exceed the total stress by a significant amount showing that the clay has finite tensile strength. After the pressure peak, the gas pressure under constant volume conditions is close to the average total stress. This suggests that the sharp pressure drop after the peak is the result of a breakdown of the tensile strength of the bentonite.

Abrupt drops in gas injection pressure, accompanied by similar drops in total stress, can be interpreted as fracture propagation events. The first fractures that form in the clay may not intersect the gas sinks. Additional gas pressure is often needed to produce fully-conductive fractures which connect with the sinks.

When the test geometry provides a number of possible gas sinks, it is found that gas outflows are always non-uniformly distributed between these sinks. The distribution of flow often changes abruptly and spontaneously during the course of an experiment. The experimental evidence is consistent with the development of a relatively small number of gas pathways through the clay. Gas conductive pathways are clearly very unstable.

When gas injection is stopped, the gas pressure and rate of outflow spontaneously decline with time. The pressure transient approaches an asymptote which coincides with the zero flow rate condition. The gas pressure at the asymptote (shut-in pressure) represents the minimum pressure at which gas is mobile in the clay. During a shut-in, the gas pressure exceeds the monitored porewater pressure by an amount equal to the capillary pressure. The decline in gas pressure during a post-peak transient reflects a similar decline in the internal porewater pressure. In constant volume tests, the capillary pressure has a value which is close to the measured swelling pressure.

Shut-in pressures for the constant volume and radially-constrained (K_0) boundary conditions are of similar magnitude and both tend to be larger than the shut-in pressure measured under constant total stress boundary condition. These tests are distinguished by the amount of dilatancy that the specimen can undergo. It is clear that dilatancy under undrained constant volume conditions is limited to elastic compression of water and minerals The shut-in pressure under constant stress is probably lower than that under other boundary conditions because the specimen is able to undergo inelastic dilatancy in the direction perpendicular to the axis of flow.

5.1 Peak gas pressure

According to the 'classic theory' of hydrofracture /Haimson and Fairhurst, 1967/, a tensile fracture will develop and propagate when the tensile effective stress acting in a direction tangential to the cylindrical surface of the source filter is equal to the tensile strength, T, of the clay. Using linear elastic stress analysis, the gas fracturing pressure of the clay around the filter is given by

$$p_g\,(\text{peak}) = T + 2\sigma_{eff} + p_w \qquad 5\text{-}1$$

where σ_{eff} is the isotropic effective stress outside the region of stress concentration and p_w is the porewater pressure in the clay. For saturated bentonite, the isotropic effective stress must be equal to the swelling pressure. The appropriate value for the porewater pressure in the CVRF test is the magnitude of this quantity just before the main gas breakthrough event. For test Mx80-10, we have p_w = 7.7 MPa. Substituting σ_{eff} = 5.5 MPa and T = 2.7 MPa gives a gas fracturing pressure p_g (peak) = 21.4 MPa, which compares favourably with the peak gas pressure of 22.1 MPa measured in this test.

In the post-peak region, the fracture will lie beyond the region of stress concentration around the filter and the bentonite will have lost its tensile strength normal to the plane of the fracture. The gas pressure is now equal to the total stress, σ, as illustrated by Figure 5-1. On this basis, the gas pressure at any point on the post-peak transient can be written as:

$$p_g\,(\text{post} - \text{peak}) = \sigma = \sigma_{eff} + p_w \qquad 5\text{-}2$$

Referring to Figure 4-20, at an elapsed time of 145 days we have σ_{eff} = 5.5 MPa and p_w = 10.8 MPa. The predicted post-peak gas pressure is therefore 16.3 MPa, which is very close to the measured value of 16.1 MPa. By way of a comparison, the average total stress on the specimen at this same time was 15.8 MPa. It is clear from Equation 5-2 that the shape of the post-peak pressure transient is governed by the couple between gas pressure and porewater pressure. It is not yet possible to reconcile the behaviour under the constant stress boundary condition of earlier tests with the classic hydrofracturing concepts outlined above.

5.2 Post-peak and near steady-state behaviour

The (near) steady-state flow condition at fixed pumping rate is defined when the rate of change of gas injection pressure is essentially zero, acknowledging the limitations in determining this rate imposed by measurement resolution and the experimental timescale.

At the (near) steady-state condition, the gas permeability of the fracture network must remain more or less constant with time, with no tendency for crack dilation or closure. Conceptually, the fracture must be propped open at any point along its length by the local gas pressure. Under constant volume conditions, mechanical equilibrium of forces demands that the total stress be moderately homogeneous throughout the clay. Any variability will be governed by shear strength. The stress sensors in test Mx80-10 show a maximum variability at the walls of the pressure vessel of around 3 MPa.

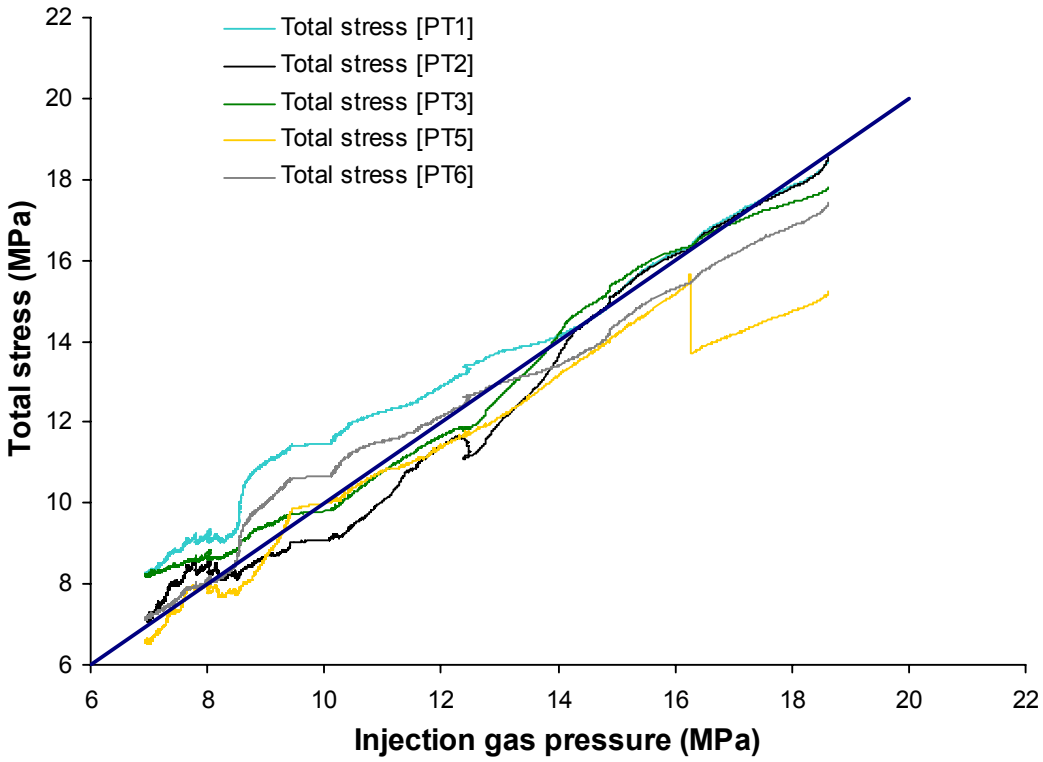

Figure 5-1. *Cross-plot from test history Mx80-10 showing total (boundary) stress and remote porewater pressure plotted against the injection gas pressure. This data covers the period from the first major gas breakthrough event (around 140 days) to the end of the first shut-in stage at 507 days.*

Given that total stress must be moderately homogeneous and a conductive fracture must be propped by gas, the gradient of the gas pressure cannot be significantly larger than around 3 MPa over the distance separating the source and sink filters. Furthermore, the internal porewater pressure gradient between the source and the sink must be similar to the gas pressure gradient.

The existence of a porewater pressure gradient in the clay would tend to suggest some drainage of water to the sink filters during (near) steady-state gas flow. The underlying mechanism has been identified as pressure-induced consolidation of the clay mass. Under constant volume conditions, any consolidation would be accompanied by a decrease in the degree of saturation. It seems possible that such a decrease could lead to a gradual increase in the permeability to gas. This might call into question the uniqueness of the values of (near) steady-state pressure quoted in this report. However, evidence presented below indicates that there was no measurable decrease in saturation during gas testing.

5.3 Capillary pressure

The capillary pressure, p_c, of the clay is the difference between the gas pressure, p_g, and the water pressure, p_w, or:

$$p_c = p_g - p_w \qquad 5\text{-}3$$

Taking the average value for this difference over 170 days of the shut-in stage of Mx80-10 gives a capillary pressure of 5.8 MPa, quite close to the measured values of swelling pressure and shut-in pressure. Equation 5-2 can be re-written as

$$\sigma_{eff} = p_g\,(\text{post} - \text{peak}) - p_w \qquad 5\text{-}4$$

which shows immediately that the capillary pressure over the entire post-peak history is equal to the effective stress in the clay. Since the effective stress can be equated with the swelling pressure, this leads to the general conclusion that the capillary pressure of bentonite close to full saturation is equal to the swelling pressure, as was suggested by the second author in /Rodwell et al, 1999/.

5.4 Shut-in behaviour

When gas injection is stopped, gas pressure drops rapidly and then gradually falls away along a very protracted pressure transient. Under constant volume conditions, the gas pressure and total stress are approximately equal at all points along the transient.

As gas pressure decreases, individual flow pathways should collapse leading to declining overall gas permeability. Under constant volume conditions, the gas pressure cannot fall below the sum of the capillary pressure, p_c, and the externally-applied water pressure (backpressure), p_{we}, or:

$$p_g\ (\text{shut - in}) = p_c + p_{we} \qquad 5\text{-}5$$

This provides a lower bound value for the gas pressure at shut-in. Taking p_c = 5.8 MPa and p_{we} = 1.0 MPa gives a lower bound value of 6.8 MPa. Independent measurements from CVRF testing give shut-in pressures of 8.0 and 7.0 MPa. It would therefore appear to be the case that flow pathways cease to be conductive at a gas pressure slightly larger than this theoretical minimum value.

5.5 Self-sealing

Strong evidence is presented here that gas flows through a network of pressure-induced pathways. Very little, if any, displacement of water occurs during gas movement. The crack-like pathways are propped open by the elevated gas pressure. When gas pressure falls, individual pathways can snap shut leading to a reduction in overall gas permeability. In the CVRF tests, spontaneous changes in the slope of the pressure transients and temporal variations in the amount of gas discharged to sinks collectively demonstrate the unstable nature of the pathways. There is also evidence from Mx80-10 that the clay regained some of its tensile strength during the rehydration phase. Spontaneous closure of gas conducting pathways and re-establishment of strength in tension can each be interpreted as a capacity for ‘self-sealing’.

6 Conclusions

Gas pressure under constant volume conditions can rise to exceed the total stress by a significant amount, showing that the clay has finite tensile strength. After the pressure peak, the gas pressure under constant volume conditions is close to the average total stress. The sharp pressure drop after the peak is indicative of a breakdown in the tensile strength of the bentonite. Abrupt drops in gas injection pressure, accompanied by similar drops in total stress, can be interpreted as fracture propagation events. The first fractures that form in the clay may not intersect the gas sinks. Additional gas pressure is often needed to produce fully-conductive fractures which connect with the sinks.

The experimental evidence is consistent with the development of a relatively small number of crack-like pathways through the clay. When multiple sinks are provided, the outflow of gas is always non-uniformly distributed between the sinks. Furthermore, the distribution of flow between sinks often changes abruptly and spontaneously during the course of an experiment. The gas pathways are clearly very unstable.

Gas entry and breakthrough under constant volume boundary conditions causes a substantial increase in the total stress acting on the clay and the internal porewater pressure. It is possible to determine the point at which gas enters the clay by monitoring changes in these parameters.

The observation that gas entry, breakthrough, peak and steady-state gas pressures are sensitive to test boundary conditions tends to confirm that gas entry is accompanied by dilation of the bentonite fabric (i.e. there is a tendency for the volume of the specimen to increase). Breakthrough and peak pressures may also be affected by the number, location and geometry of the sink filters and by the rate of gas pressurisation.

When gas injection is stopped, the gas pressure and rate of outflow spontaneously decline with time. The gas pressure at the asymptote (shut-in pressure) represents the minimum pressure at which gas is able to move in the clay. During a shut-in, the gas pressure exceeds the internal porewater pressure by an amount equal to the capillary pressure. The decline in gas pressure during a post-peak transient reflects a similar decline in the porewater pressure in the clay. In constant volume tests, the capillary pressure has a value which is close to the measured swelling pressure.

The swelling pressure of the buffer clay at a dry density of 1.58 $Mg.m^{-3}$ was determined to be around 5.5 MPa. Hydraulic testing under constant volume conditions gave an average permeability of 1.4×10^{-21} m^2. For conditions of varying externally-applied porewater pressure, p_w, the average total stress, σ, acting on the walls of the pressure vessel is given by the relationship

$$\sigma = \Pi + \alpha\, p_w \qquad 6\text{-}1$$

where $\alpha \approx 0.86$ for increasing water pressure and $\alpha \approx 0.75$ for decreasing pressure. Possible reasons for $\alpha \neq 1$ and the observed hysteretic behaviour include side-wall friction between the clay and the steel vessel, the presence of small residual air bubbles in the clay at the onset of testing, and the finite compliance of the sensors used to measure the total stress.

What is absolutely clear from these gas injection experiments is that it is possible to pass up to 60 litres (STP) of helium through specimens of buffer clay (at gas pressures of over 8.0 MP for times in excess of 5 months) without any measurable desaturation occurring. This strongly reinforces the observations made by others on the lack of desaturation occurring during gas flow through fully-hydrated bentonite.

After intense scrutiny of the experimental data, we are unable to present any convincing evidence of porewater displacement, desaturation or conventional two-phase flow in buffer bentonite. Nevertheless, a case can be made for some degree of bentonite dewatering by internal consolidation of the clay when the gas pressure acting within the buffer exceeds the sum of the swelling pressure and the external water pressure.

There is no evidence from these tests that the development of pressure-induced gas pathways in any way compromises the sealing capacity of the bentonite barrier. Gas pathways are ephemeral features of the buffer which tend to close up when gas pressure falls. Breaks in slope of monitored pressure transients can be interpreted as discrete pathway 'sealing' events which coincide with decreases in the rate of discharge of gas to the sinks. More importantly, a history of gas movement through the buffer has been shown to have no detectable effect on permeability to water.

Since our current knowledge of buffer gas flow is based exclusively on small-scale laboratory tests, the key question of scale dependency has yet to be addressed. Future work might therefore include a full-scale field simulation of buffer gas migration.

7 References

Donohew A T, Horseman S T, Harrington J F, 2000. Gas entry into unconfined clay pastes between the liquid and plastic limits. Chapter 18. In: Environmental Mineralogy – Microbial Interactions, Anthropogenic Influences, Contaminated Land and Waste Management (eds J.D. Cotter-Howells, L.S. Campbell, E. Valsami-Jones and M. Batchelder), Mineralogical Society, London, Special Publication No. 9, 369–394.

Fleureau J-M, Kheirbek-Saoud S, Soemitro R, Taibi S, 1993. Behaviour of clayey soils on drying-wetting paths. Canadian Geotechnical Journal, Vol. 30, 287–296.

Gallé C, 1995. Etudes de la migration du gaz hydrogène (H_2) dans l'argile Fo-Ca. Etude préliminaire. Technical Report CEA DESD/95.135, Saclay, France.

Gallé C, 1998. Migration des gaz et pression de rupture dans une argile compactée destinée à la barrière ouvragée d'un stackage profound. Bulletin Soc. Géol. France, Vol. 169, Part 5, 675–680.

Gray M, Kirkham T J, Lin A W-L, Graham J, 1996. On the gas breakthrough resistance of engineered clay barrier materials proposed for use in nuclear fuel waste disposal. In: Proc. CNS Int. Conf. on Deep Disposal of Radioactive Waste, Canadian Nuclear Society, Winnipeg, Manitoba, 16–19 Sept.

Haimson B C, Fairhurst C, 1967. Initiation and extension of hydraulic fractures in rock. Journal of the Society of Petroleum Engineers (SPE), Sept., 310–318.

Harrington J F, Horseman S T, 1999. Gas transport properties of clays and mudrocks. In: Muds And Mudstones: Physical And Fluid Flow Properties (eds A.C.Aplin, A.J. Fleet, and J.H.S. Macquaker). Geological Society of London, Special Publication No. 158, 107–124.

Harrington JF, Hoseman S T, Noy D J, 2001. Swelling and osmotic flow in a potential host rock. In: Proc 6th International Workshop on Key Issues in Waste Isolation Research. Held in Paris, France. 28th–30th November 2001. Special edition of Engineering Geology.

Harrington J F, Horseman S T, Sellin P, 2002. Gas flow in buffer bentonite under constant volume conditions. In: Proc. Workshop on the Clay Microstructure and its Importance to Soil Behaviour, Lund, Sweden, 15–17 Sept., 41–57.

Hokari T, Okihara M, Ishii T, Ikuse H, 1997. Experimental study on scale effects of bentonite/sand mixtures on gas migration. In: Proc. Scientific Basis For Nuclear Waste Management XX, Boston, 2–6 Dec., 1996 (eds W.J. Gray And I.R. Triay), MRS Symposia Proceedings, Vol. 465, Materials Research Society, Warrendale, Pennsylvania, 1019–1026.

Horseman S T, 1996. Generation and migration of repository gases: Some key considerations in radioactive waste disposal. In: Proc. Int. 2-Day Conference, London, 21–22 Nov. 1996, IBC Technical Services, Energy Division, 26 pp.

Horseman S T, Harrington J F, 1997. Study of gas migration in Mx80 buffer bentonite British Geological Survey, Technical Report WE/97/7.

Horseman S T, Harrington J F, Sellin P, 1997. Gas Migration In Mx80 Buffer Bentonite. In: Proc. Scientific Basis For Nuclear Waste Management XX, Boston, 2–6 Dec., 1996 (eds W.J. Gray And I.R. Triay), MRS Symposia Proceedings, Vol. 465, Materials Research Society, Warrendale, Pennsylvania, 1003–1010.

Horseman S T, Harrington J F, Sellin P, 1999. Gas migration in clay barriers. Engineering Geology, Vol. 54, 139–149.

Hume H B, 1999. Gas breakthrough in compacted Avonlea bentonite. MSc thesis, Department of Soil Science, University of Manitoba, Winnipeg, Canada.

Johannesson L-E, Börgesson L, Sandén T, 1995. Compaction of bentonite blocks: Development of technique for industrial production of blocks which are manageable by man. Svensk Kärnbränslehantering AB, TR 95-19.

Kirkham T, 1995. Development of test equipment and procedures for determination of the gas-breakthrough pressure of compact clay materials with preliminary results. MSc thesis, Department of Civil and Geological Engineering, University of Manitoba, Winnipeg, Canada.

Lambe T W, Whitman R V, 1969. Soil Mechanics, John Wiley & Sons Inc.

Pusch R, Forsberg T, 1983. Gas migration through bentonite clay. SKB Technical Report 83-71, Stockholm, Sweden.

Pusch R, Ranhagen L, Nilsson K, 1985. Gas migration through Mx-80 bentonite. Nagra Technical Report NTB 85-36, Wettingen, Switzerland.

Pusch R, Hökmark H, Börgesson L, 1987. Outline of models of water and gas flow through smectite clay buffers. SKB Technical Report 87-10, Stockholm, Sweden.

Rodwell W R, Harris A W, Horseman S T, Lalieux P, Müller M, Ortiz Amaya L, Pruess K, 1999. Gas migration and two-phase flow through engineered and geological barriers for a deep repository for radioactive waste. EC/NEA Status Report EUR 19122EN, European Union, Luxembourg.

Tanai K, Kanno T, Gallé C, 1997. Experimental study of gas permeabilities and breakthrough pressures in clays. In: Scientific Basis For Nuclear Waste Management XX, Boston (eds W.J. Gray And I.R. Triay), MRS Symposia Proceeding Vol. 465, Materials Research Society, Warrendale, Pennsylvania, 1003–1010.

8 Acknowledgements

The authors wish to thank Dr David Noy, developer of the FESTIG 3-D finite element groundwater flow code, for his assistance in numerically modelling the hydraulic permeability stages of the test programme. Mr Humphrey Wallis and staff of the BGS R&D Workshops are thanked for their technical skills and excellent workmanship in the manufacturer of the pressure vessels. Thanks are also expressed to Mr Shaun Reeder for carefully proof-reading the manuscript prior to publication.

ISSN 1404-0344

CM Digitaltryck AB, Bromma, 2003